

AgroCoT: A Chain-of-Thought Benchmark for Evaluating Reasoning in Vision-Language Models for Agriculture

Yibin Wen^{1,*} Qingmei Li^{2,*} Zi Ye^{1,*} Jiarui Zhang^{1,*} Zurong Mai¹
 Jing Wu¹ Shuohong Lou¹ Yuhang Chen¹ Henglian Huang¹
 Xiaoya Fan³ Yang Zhang¹ Defeng Gu¹ Lingyuan Zhao⁴ Yutong Lu^{1,7}
 Haohuan Fu^{2,7} Jianxi Huang^{5,6} Juepeng Zheng^{1,7,†}

¹Sun Yat-sen University ²Tsinghua University ³Southwest University

⁴HuanTian Wisdom Technology Co., Ltd. ⁵China Agricultural University

⁶Southwest Jiaotong University ⁷National Supercomputing Center in Shenzhen

*Equal contribution †Corresponding author

Abstract. Recent advancements in Vision-Language Models (VLMs) have significantly impacted various industries. In agriculture, these multimodal capabilities hold great promise for applications such as precision farming, crop monitoring, pest detection, and environmental sustainability. However, while several Visual Question Answering (VQA) datasets and benchmarks have been developed to assess VLM performance, they often fail to effectively evaluate the critical reasoning and problem-solving skills needed in complex agricultural contexts. To address this gap, we introduce AgroCoT, a VQA dataset that integrates Chain-of-Thought (CoT) reasoning, specifically designed to evaluate the reasoning capabilities of VLMs. With 4,759 carefully curated samples, AgroCoT provides a comprehensive and robust evaluation of reasoning abilities, particularly in zero-shot scenarios, focusing on the models' ability to engage in logical reasoning and effective problem-solving. Our evaluation of 30 representative VLMs, including both proprietary and open-source models, reveals a gap in their reasoning capabilities, which underscores the importance of incorporating CoT for assessments. Our dataset is available at <https://huggingface.co/datasets/wenyb/AgriCoT>.

Keywords: AgroCoT · Vision-language model · Chain-of-Thought benchmark · Agriculture · Visual question answering

1 Introduction

Agriculture, the cornerstone of global food security and economic stability, underpins human livelihoods and plays a central role in achieving Sustainable Development Goal 2 (Zero Hunger) [36]. However, it now faces unprecedented challenges from climate extremes and land degradation. Recent advancements in Artificial Intelligence, particularly Large Language Models (LLMs) and Vision-Language Models (VLMs), offer promising solutions to agricultural challenges,

including crop disease diagnosis [6, 51, 58], pest management [53, 54, 56], and precision farming [5, 46]. Although existing VLMs (such as GPT-5 [21], Qwen2.5-VL [4], etc.) demonstrate exceptional generalization across diverse visual and textual tasks and show significant promise in comprehensive agricultural applications, the effectiveness of these VLMs in agricultural scenarios requires careful evaluation to help researchers select the most appropriate models for purposes.

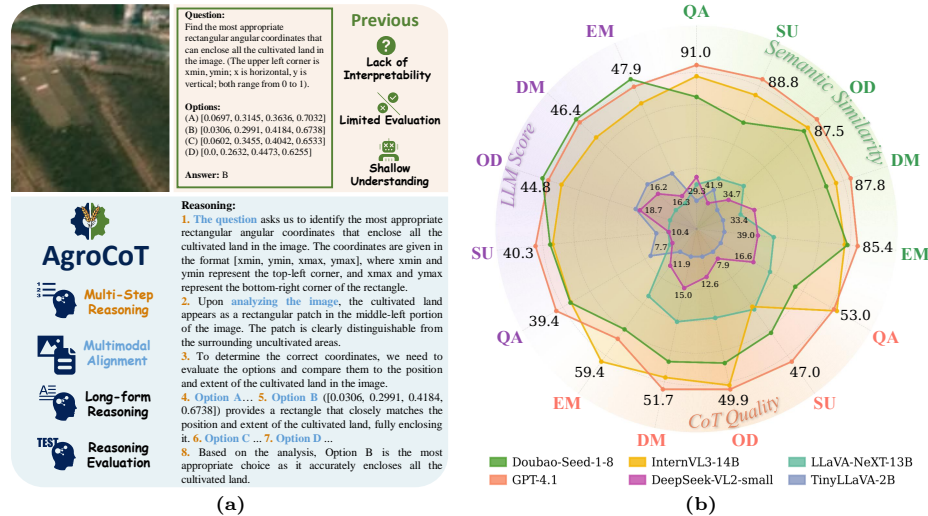


Fig. 1: (a) illustrates the advantages of AgroCoT over existing benchmarks, while (b) presents an overview of VLM performance across multiple evaluation dimensions.

Recently, several multimodal benchmarks have been developed for agricultural applications. These benchmarks [11, 14, 37] incorporate images from the Internet or existing agriculture dataset, and texts from user-expert interactions, authentic dialogues or synthetic data. For example, CDDM [27] creates a benchmark for crop disease diagnosis and AgroMind [22] focuses on agricultural remote sensing scenarios. To provide a straightforward assessment of how well VLMs can answer agricultural questions, existing benchmarks typically adopt various question-answering formats and rely on accuracy-based metrics.

However, existing agriculture-related benchmarks only offer a limited assessment of VLMs' capabilities (see Fig. 1 (a)), resulting in poor interpretability, limited evaluation, and shallow understanding. This motivates a more comprehensive benchmark that evaluates internal abilities to analyze problems, understand scenarios, and perform multi-step reasoning. By breaking down complex multimodal tasks into clear steps, Chain-of-Thought (CoT) reasoning [13, 16, 45, 55] has been shown to improve the interpretability, depth of reasoning, and generalization capabilities of VLMs. At the same time, it mitigates the black-box nature of these models [30], reduces the likelihood of hallucinations, and aligns the model's reasoning process with expert decision-making workflows. To the best

of our knowledge, there is no benchmark available to assess a model’s multi-step reasoning abilities in the agricultural domain.

Considering the limitations of the aforementioned benchmarks and the current developmental needs of general VLMs in agricultural scenarios, we propose a new benchmark for multi-step multimodal Chain-of-Thought in agriculture, called AgroCoT. To the best of our knowledge, AgroCoT is the first comprehensive VQA benchmark in the agricultural domain that incorporates explicit CoT reasoning. As shown in Fig. 1 (a), AgroCoT introduces four key advantages: multi-step reasoning, multimodal alignment, long-form reasoning and reasoning evaluation, which is designed to deeply assess the problem-solving and reasoning capabilities of existing representative VLMs, thereby exposing the weaknesses of current VLMs and offering a direction for future model improvement. As shown in Fig. 1 (b), our evaluation results indicate that existing VLMs may fall short in their reasoning capabilities, highlighting their limitations towards agricultural understanding and decision-making with multi-step and long-form reasoning.

Overall, the primary contributions of this work can be summarized as follows:

- We propose AgroCoT, a comprehensive agricultural multi-step, multimodal CoT dataset comprising 4,759 VQA pairs. Each pair includes human-refined CoT reasoning, which allows for a comprehensive evaluation of models’ understanding and reasoning abilities across various agricultural contexts.
- As a problem-oriented benchmark, AgroCoT addresses five key dimensions (object detection, quantitative analysis, disease monitoring, spatial understanding, and environmental management) designed to tackle critical agricultural challenges with a total of 15 task types.
- We conduct a thorough evaluation of 25 open-source and 5 proprietary VLMs, focusing on their accuracy in answering questions as well as their reasoning abilities. Additionally, we analyze how the performance of models varied across tasks with different levels of CoT reasoning steps.

2 Related Work

2.1 Large Vision-Language Models

Vision-Language Models (VLMs) that couple visual encoders with large language models have rapidly advanced general-purpose multimodal understanding [24], with CLIP [33] establishing scalable vision-language representations for strong zero-shot transfer. Proprietary models like GPT-4o [1] and Gemini [39] push multimodal reasoning at scale, while open-weight models such as DeepSeek [25] and Qwen-VL [3] lower the barrier for domain adaptation in specialized applications.

Adapting VLMs to agriculture shows promise but also reveals gaps. Domain-specific initiatives include AgroGPT [2] for agricultural VQA, Agri-LLaVA [41] for crop disease diagnosis, and vision-language pipelines for crop health monitoring, disease recognition [51] or parcel segmentation [46]. However, these models are often trained and evaluated on crop- or symptom-specific datasets with limited scenes and sensors [27, 51], and current evaluations rarely cover practical

skills such as counting, planting recommendations or environmental management. Therefore, there is an urgent need for a benchmark that spans a broader range of agricultural scenes across multiple sensing platforms, so that the capabilities of models can be assessed more faithfully in real-world field conditions.

2.2 Chain-of-Thought

Chain-of-Thought (CoT) [43] helps large models solve complex problems by breaking them into intermediate steps. Simple prompts can elicit stepwise reasoning and improve performance on arithmetic, commonsense, and logic tasks [19, 20, 45]. Reliability is further enhanced through self-consistency voting [42] and systematic search over intermediate states [48]. In multimodal settings, textual rationales should align with visual evidence [38], as in ScienceQA [30], which pairs images, questions, and human-written rationales to supervise step-by-step reasoning. Compositional CoT [31] uses scene-graph intermediates, and Interleaved-modal CoT [12] inserts attention-selected regions.

Despite this progress, multimodal CoT benchmarks [13, 15, 19, 23, 32, 44, 52] remain limited in reasoning depth, image diversity, and domain coverage. ScienceQA [30] targets K-12; MMMU [49] and MathVista [29] emphasize cross-disciplinary and visual mathematics without explicit long-chain annotations; AOKVQA [34] offers training or multiple-choice rationales but does not evaluate generated intermediate steps at scale; M³CoT [7] and MME-CoT [19] enforce multi-domain, multi-step, multimodal reasoning but do not cover agriculture. This reveals a core limitation for agricultural multimodal reasoning: the absence of a benchmark with detailed CoT for qualitative assessment. Motivated by this, we introduce explicit, structured CoT for agricultural scenarios, which enables evaluation of the CoT generated by models and provides deeper insights into how well models understand and analyze complex agricultural problems.

2.3 Agriculture Benchmark for VLMs

Tab. 1 summarizes the variety of existing benchmarks developed in recent years to evaluate VLM capabilities in agricultural domain. Some datasets such as AGMMU [14] and AgroBench [37] focus on general VQA to assess a model’s comprehension of agricultural scenes. More recently, AgroMind [22] introduces a comprehensive benchmark with multi-sensor imagery to evaluate models on complex tasks like spatial perception and scene reasoning. AgriBench-VL-4K [47] is a comprehensive and challenging benchmark, featuring multi-metric evaluation and a dual evaluation framework. Complementing these general evaluations, other datasets address more specific applications. For instance, AgroInstruct [2] facilitates expert-level instruction tuning, MIRAGE [11] explores multi-turn conversational interactions like expert consultations, and CDDM [27] provides a large-scale multimodal dataset, but only for crop disease diagnosis. In contrast, some datasets like CROP [50] have focused on enhancing language models for crop science but are text-based and do not incorporate visual input.

Table 1: Comparison of AgroCoT with existing agriculture datasets and benchmarks. CoT shows whether the dataset contains Chain-of-Thought reasoning. Abbreviations adopted: #Q for the number of questions; MCQ for Multiple Choice Questions; TFQ for True-or-False Questions; OEQ for Open-Ended Questions; LFQ for Long-Form Question-answering; Conv for Conversational multi-turn interactions. AgroCoT is the only dataset in the agricultural domain that contains CoT.

Dataset	#Q	Answer Type	Multimodal	Multi-view	CoT
CROP [50]	5,045	MCQ	✓	✓	✓
CDDM [27]	1 million	TFQ, OEQ	✓	✓	✓
AgroInstruct [2]	70 K	TFQ, OEQ	✓	✓	✓
MIRAGE [11]	41 K	LFQ, Conv	✓	✓	✓
AGMMU [14]	1,492	MCQ, OEQ	✓	✓	✓
AgroBench [37]	4,342	MCQ	✓	✓	✓
AgriBench-VL-4K [47]	3,876	MCQ, OEQ	✓	✓	✓
AgroMind [22]	28,482	MCQ, TFQ, OEQ	✓	✓	✓
AgroCoT (Ours)	4,759	MCQ, TFQ, OEQ, LFQ	✓	✓	✓

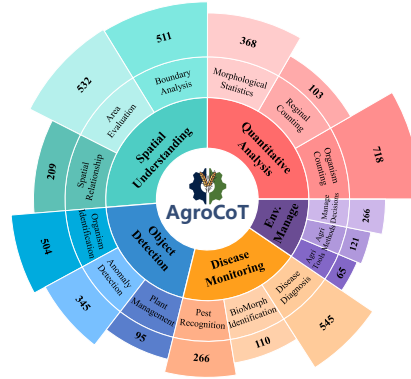


Fig. 2: The number of samples across different dimensions in AgroCoT.

Despite these advancements, existing agricultural benchmarks primarily evaluate models based on final answer accuracy and offer limited question types, as summarized in Tab. 1. Additionally, none of these benchmarks incorporate explicit CoT reasoning. To address these gaps, we present AgroCoT, a multimodal, multi-view benchmark that encompasses diverse agricultural scenarios. Each item includes a human-refined, multi-step CoT, enabling joint evaluation of answer correctness and reasoning quality.

3 AgroCoT

AgroCoT is a multimodal benchmark designed for agriculture. It is a VQA dataset enriched with CoT reasoning and includes 4,759 VQA pairs, whose scale is consistent with modern multimodal benchmarks (*e.g.*, MME-CoT [19]: 1,130 samples; CoMT [9]: 3,853 samples). As illustrated in Fig. 1 (b), AgroCoT allows for the assessment of reasoning abilities by evaluating not only the accuracy of the final answers but also the depth and coherence of the reasoning processes involved, ensuring a thorough analysis of their agricultural reasoning capabilities.

3.1 Problem-Oriented

As a problem-driven multimodal benchmark specifically designed for agricultural applications (see Fig. 2 and Fig. 3), AgroCoT is organized around five key real-world problem types: Object Detection (**OD**), Quantitative Analysis (**QA**), Disease Monitoring (**DM**), Spatial Understanding (**SU**), and Environmental Management (**EM**), commencing with foundational identification, advancing through quantitative assessment and diagnostic scrutiny, and culminating in sophisticated spatial reasoning and decision-making support. These five

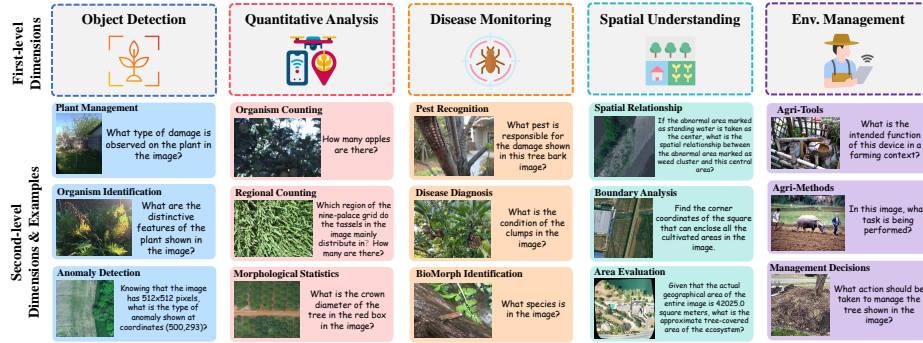


Fig. 3: Hierarchical task system of AgroCoT. Based on the progressive cognitive pipeline in agricultural intelligence, AgroCoT constructs five evaluation dimensions (such as object detection, quantitative analysis, disease monitoring, spatial understanding and environmental management), covering 15 different and diverse task types.

areas form a systematic hierarchy of agricultural cognition, progressing from fundamental visual perception (OD, SU) to domain-specific analytical reasoning (QA, DM) and ultimately to high-level decision-making (EM).

Object Detection forms the foundation of agricultural visual understanding by identifying and localizing key entities and anomalies in field images. Key tasks at this level include Plant Management, covering plant management by providing control and optimization strategies; Organism Identification, focusing on identifying organisms such as crops, plants, leaves, fruits, *etc.*, addressing core questions like “what is it?”; and Anomaly Detection, detecting anomalies in planting and environmental issues (*e.g.*, waterlogging), and analyzing spatial relationships between anomalies.

Quantitative Analysis targets precise measurement and enumeration to support data-driven agronomic decisions. This includes Organism Counting, addressing counting organisms like insects and individual crops to obtain population data; Regional Counting, targeting in specific areas such as nine-grid divisions or corners; Morphological Statistics, measuring parameters (*e.g.*, crown diameter), counting fruit sizes, and quantifying spatial units in parcels.

Disease Monitoring goes beyond detection to diagnose health status and recommend interventions based on visual symptoms. Typical tasks include Pest Recognition, which involves identifying pests and assessing their impact on crops or other organisms; BioMorph Identification, which focuses on identifying insects or plants, emphasizing species or traits without diagnosing diseases; and Disease Diagnosis, which centers on diagnosing crop health (*e.g.* leaves), identifying disease types with diseases, symptoms, and management solutions.

Spatial Understanding represents the geometric reasoning layer, enabling boundary definition, area quantification, and spatial relationship. Tasks in this dimension include Boundary Analysis, which focuses on analyzing the boundaries of targets such as farmland, including coordinate matching and bounding box solutions; Area Evaluation, which encompasses area estimates, ratios, coverage

assessments, and level descriptions; and Spatial Relationship, which involves tasks such as analyzing spatial relationships between anomalous regions and developing resource optimization strategies based on weed or crop coverage.

Environmental Management integrates contextual knowledge of tools, practices, and terrain to guide adaptive farm operations. This includes Agri-Tools, identifying agricultural tools, equipment, or structures, clarifying their names, functions, and attributes; Agri-Methods, revolving around operational processes, traditional practices, and addressing types; Management Decisions involving determining environmental attributes (*e.g.*, climate zones or terrain) and formulating management decisions for crops, weeds, or trees.

3.2 CoT Reasoning

Compared to traditional VQA benchmarks in the agriculture, AgroCoT introduces a significant innovation of the CoT reasoning process. For each VQA sample (see Fig. 1 (a)), the reasoning steps follow a structured sequence: (1) understanding the question, (2) describing the image, (3) retrieving relevant knowledge to connect the question and image, (4) logically reasoning toward an answer, and (5) providing the final response. The length and complexity of the reasoning chain vary depending on the task. For instance, in text-based multiple-choice questions, the model explains each option individually, while for image-based questions, the reasoning process involves a detailed description of each image. This flexibility ensures that the reasoning chain is comprehensive and adaptable to different question types.

The incorporation of CoT reasoning addresses a key limitation of traditional agricultural VQA datasets, which typically focus on end-to-end evaluations without explicitly considering the reasoning process. Such datasets primarily assess the ability to retrieve relevant knowledge rather than evaluate the depth of their reasoning. In contrast, AgroCoT advances the evaluation process by providing deeper insights into the reasoning capability, showcasing how well it understands and interprets agricultural scenarios. This evaluation highlights specific weaknesses in the reasoning process, allowing researchers to enhance VLMs for more accurate and reliable applications in agriculture.

4 Dataset

4.1 Data Construction

Data Sources. To address the persistent challenges in agricultural scenarios, we construct a comprehensive benchmark for evaluating VLMs. As illustrated in Fig. 4, we curate four representative datasets—CDDM [27], AgMMU [14], AgroMind [22], and AgroBench [37]—and further introduce a proprietary VQA dataset developed in this work to ensure diverse and comprehensive evaluation.

Each dataset contributes complementary strengths toward addressing key agricultural challenges. CDDM [27] provides a large-scale collection of crop disease images paired with diagnostic questions, supporting disease monitoring

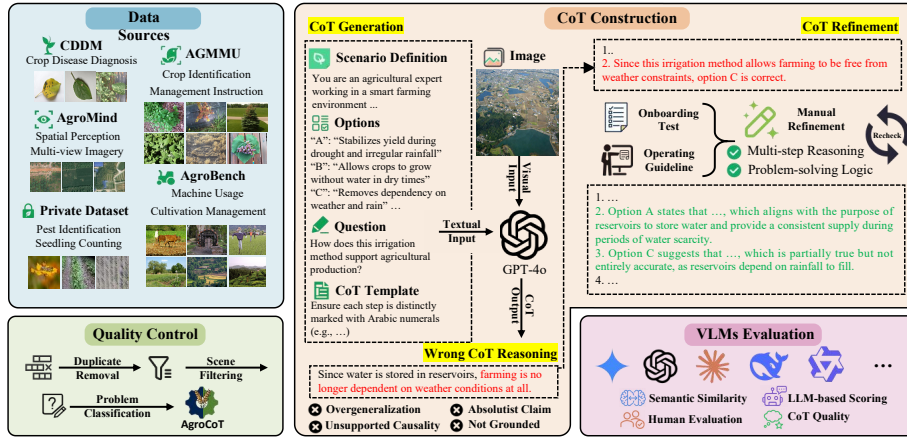


Fig. 4: The construction of AgroCoT benchmark with four steps: collecting samples from data sources, ensuring the quality of the samples, generating a CoT for each QA pair, and conducting a comprehensive evaluation of the representative VLMs.

tasks. AgMMU [14] emphasizes species identification, pest and disease classification, and agricultural management, enriching AgroCoT with object detection and environmental management scenarios. AgroMind [22] integrates multi-sensor imagery from ground cameras, UAVs, and remote sensing platforms, facilitating quantitative reasoning and spatial analysis. AgroBench [37] contributes decision-oriented questions related to disease management and agricultural tool usage, which are essential for practical agricultural operations. Appendix 1 provides a more detailed introduction to the dataset’s sources, proportions, filtering process, and global distribution characteristics.

In addition, our proprietary dataset supplements fine-grained tasks such as pest identification and seedling counting, which remain underrepresented in existing benchmarks. Collectively, these datasets expand scenario coverage and task diversity, providing a comprehensive evaluation platform for assessing model generalization under real-world agricultural production conditions.

Quality Control. To ensure both diversity and relevance, we remove duplicates and apply scenario filtering to prioritize more complex reasoning tasks, while retaining a subset of simpler knowledge-based questions to maintain balance. We further structure the collected dataset around the practical demands of current agricultural tasks, thereby constructing a problem-driven benchmark tailored for rigorous evaluation of VLMs in agricultural applications.

CoT Generation. Building upon the curated VQA dataset, we utilize GPT-4o [18] to pre-generate an initial CoT for each sample. The primary inputs to the model were the image and question, supplemented with additional context, including the definition of the agricultural scenario and a template for the reasoning format. This approach enables the model to generate the reasoning process in the specified CoT format, significantly reducing the manual effort. Appendix 2.1 presents the prompts designed to guide GPT-4o in generating CoTs.

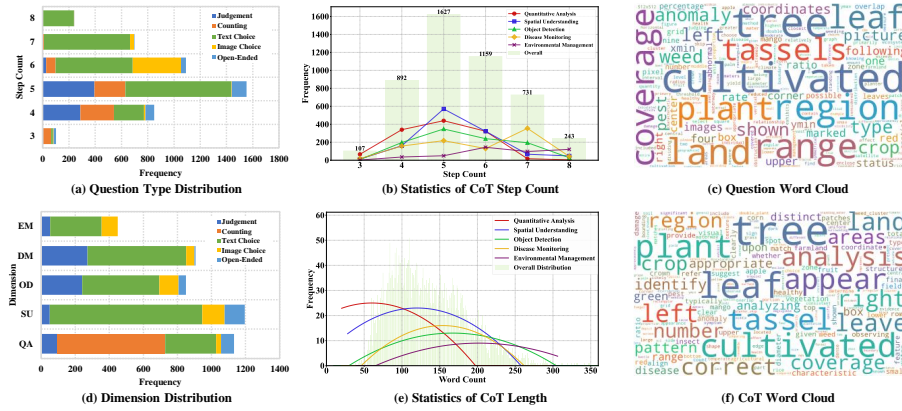


Fig. 5: Statistics of AgroCoT, from three perspectives: the distribution of question types across steps and dimensions, the number of steps and length distribution of CoTs, and word cloud analysis of both questions and CoTs.

Wrong CoT Reasoning. However, due to the limited agricultural knowledge and occasional misinterpretation of the format, some erroneous outputs were generated. We identify CoTs with incorrect answers, those with correct answers but insufficient text length, as well as CoTs exhibiting issues such as inadequate depth of reasoning, format inconsistencies, missing image elements, and logical errors. These problematic CoTs are then subjected to a thorough manual review process for further refinement. More details on the filtering of wrong CoTs can be found in Appendix 2.2.

CoT Refinement. To ensure the quality of the CoTs, we select reviewers with a strong foundation in agricultural knowledge, complemented by excellent logical reasoning and textual expression skills, following a rigorous onboarding test. To ensure consistency and quality, reviewers refine the CoTs based on a standardized set of operating guidelines that outline explicit criteria for issue detection and required modifications. Through this structured refinement process, each CoT is thoroughly reviewed and enhanced to meet the standards of multi-step, logical problem-solving, ensuring alignment with the expectations of the agricultural benchmark. More details can be found in Appendix 2.3.

VLMs Evaluation. Finally, we conduct a comprehensive evaluation on AgroCoT using a diverse set of representative VLMs, covering both proprietary and open-source models, such as GPT [1], Gemini [39], Qwen-VL [3], DeepSeek-VL [28], *etc.* To assess their performance, we employ various evaluation metrics. In addition to traditional answer-level accuracy metrics, we adopt a multi-dimensional evaluation framework that includes text semantic similarity measures, LLM-based scoring, human evaluation, and CoT quality assessment to systematically examine reasoning depth and semantic alignment.

4.2 Statistics

Distribution of Question Types. AgroCoT is a benchmark with various question types, including judgment, counting, text or image choice, and open-ended questions. As shown in Fig. 5 (a), text choice is the most common, especially at 5- and 6-step reasoning, while judgment dominates at fewer steps. Image choice and counting are more frequent at 6-7 steps, and open-ended questions appear occasionally with lower frequencies. Fig. 5 (d) further highlights text choice as the primary evaluation method, with judgment and counting more prevalent in dimensions like OD and QA.

Analysis of Reasoning Steps and Length. Fig. 5 (b) shows that most tasks peak at 5-step reasoning, indicating a moderate depth of analysis. SU and OD follow a similar trend with 4- and 5-step counts, while DM and EM require deeper reasoning, with more tasks at 6-7 steps. AgroCoT includes both simpler tasks and complex ones, enabling evaluation across different reasoning complexities. Fig. 5 (e) shows that most tasks have reasoning texts between 50 and 150 words, with shorter chains more common. SU and OD also feature shorter chains, while EM has the longest, reflecting more detailed reasoning for certain tasks. This diversity in step counts and text lengths highlights the broad coverage of agricultural tasks with varying reasoning depths.

Visualisation of High-frequency Words. Fig. 5 (c) and (f) show the word clouds for the question and CoT reasoning texts, respectively. Both clouds highlight the strong focus of AgroCoT on agricultural topics. In Fig. 5 (c), terms such as “tree”, “leaf”, “plant”, “cultivated”, “region” and “land” dominate, emphasizing key agricultural elements such as crop types, regions, and environmental factors. Similarly, in Fig. 5 (f), the prominent terms include “tree”, “plant”, “cultivated”, “land” and “tassel”, indicating that the reasoning process also heavily revolves around agricultural concepts. Additionally, words such as “analyze”, “identify”, “correct” and “pattern” suggest the focus on detailed problem-solving related to crop management and environmental conditions. Both clouds illustrate that AgroCoT is centered around agricultural scenarios in questions or reasoning.

5 Evaluation Protocol

To comprehensively assess model performance, we design a systematic evaluation framework along two complementary dimensions: final answer correctness and reasoning quality, enabling joint analysis of final prediction accuracy and intermediate reasoning processes.

Semantic Similarity. We employ the all-MiniLM-L6-v2 model from the Sentence-Transformers framework to encode both model outputs and reference CoTs into 384-dimensional dense vectors. Cosine similarity between the embeddings is computed to quantify semantic consistency.

CoT Quality. To quantify the model’s coverage of key information during the reasoning process, we draw inspiration from the MME-CoT [19] approach and propose an evaluation metric based on matching key steps in the reasoning chain.

The F1 score serves as the final CoT quality score. Let the model-generated reasoning chain contain S_{out} key steps, and the reference CoT contain S_{ref} key steps. The number of successfully matched steps between the two is denoted as S_{match} , and the following metrics are defined:

$$\text{Recall} = \frac{S_{match}}{S_{ref}}, \text{Precision} = \frac{S_{match}}{S_{out}}, \text{F1 Score} = \frac{2 \times (\text{Precision} \times \text{Recall})}{\text{Precision} + \text{Recall}} \quad (1)$$

where recall measures the coverage of key steps from the reference CoT in the model’s reasoning, precision measures the validity of each step in the model’s reasoning chain and F1 Score provides a comprehensive reflection of the quality of the model’s reasoning process.

LLM Score. To ensure the robustness of the evaluation results, we employ multiple LLMs as automatic evaluators to conduct a multi-dimensional comprehensive assessment of the model-generated reasoning chains. Specifically, we select three representative open-source models—Qwen3-8B, DeepSeek-R1-Distill-Qwen-7B, and GLM-Z1-9B-0414—and design guiding prompts based on five core dimensions: accuracy, logical coherence, effectiveness, clarity, and completeness. Each dimension is scored on a scale of 10, and the evaluators assign scores to the reasoning chain based on the prompts. Ultimately, the score for each sample is the average of the scores given by the three models across the five dimensions, resulting in the final score. This design aims to integrate different evaluation perspectives from various LLMs, reducing potential biases from a single model and enhancing the reliability of the evaluation results. The design of prompts for scoring using LLMs is provided in Appendix 3.3.

Human Evaluation. Building on the LLM evaluation, we further introduce a human evaluation mechanism aimed at expanding our understanding of the model’s reasoning quality and exploring the consistency between automatic evaluation results and human judgment. Specifically, we recruited 20 volunteers with relevant backgrounds to independently score the model-generated reasoning chains using the same evaluation criteria as the automatic evaluation. The final human score for each sample is the average of the scores provided by all volunteers. The details of human evaluation will be presented in Appendix 3.4.

In Appendix 3.1, we also introduce how to calculate accuracy, along with the commonly used ROUGE and BERTScore evaluation methods.

6 Experiments

6.1 Experimental Settings

Experiments include both proprietary models—Claude-Sonnet-4.5, Gemini-2.5-Pro [39], GPT-4.1 [1], GPT-5 [21], and Doubao-Seed-1.8 [35]—and representative open-source models, including the DeepSeek-VL2 [28], InternVL [8], LLaVA-NeXT [26], Qwen-VL [3] series, as well as GLM-4.6V [17], TinyLLaVA [57], and Llama-4-Scout [40], covering diverse parameter scales.

Closed-source models are evaluated via their official APIs, while open-source models are locally deployed using publicly available weights and standardized

Table 2: Evaluation results of representative VLMs. SS denotes Semantic Similarity, and Quality refers to the CoT quality metric. Boldface indicates the best result across all models. Peach and Lemon highlight the best and second-best results among open-source models, respectively. Llama-4-Scout denotes Llama-4-Scout-17B-16E-Instruct. All results are reported as mean (standard deviation) over three independent runs.

Model	QA		SU		OD		DM		EM		Overall	
	SS	Quality										
Proprietary Large Vision-Language Models												
Claude-Sonnet-4.5	89.93 (0.53)	48.13 (0.14)	87.16 (0.34)	42.87 (0.01)	87.49 (0.12)	47.66 (0.15)	87.32 (0.32)	47.91 (0.08)	84.81 (0.57)	46.45 (0.14)	87.81 (0.47)	46.44 (0.06)
Gemini-2.5-Pro [39]	81.35 (0.87)	42.20 (0.13)	79.43 (1.12)	33.64 (0.19)	80.63 (0.78)	40.09 (0.04)	80.75 (0.39)	34.50 (0.13)	78.45 (0.59)	37.36 (0.08)	80.30 (0.72)	38.64 (0.11)
GPT-4.1 [1]	91.05 (0.13)	51.78 (0.15)	88.82 (0.18)	46.97 (0.24)	87.45 (0.45)	49.93 (0.13)	87.84 (0.76)	51.68 (0.30)	85.40 (0.51)	48.12 (0.11)	88.59 (0.38)	49.78 (0.06)
GPT-5 [21]	76.53 (0.72)	31.36 (0.13)	74.83 (0.63)	28.10 (0.24)	74.96 (0.43)	29.33 (0.11)	74.81 (0.65)	30.56 (0.04)	73.16 (0.43)	29.59 (0.13)	75.11 (0.12)	29.78 (0.24)
Doubao-Seed-1.8 [35]	74.58 (0.13)	34.93 (0.34)	70.42 (0.09)	36.04 (0.16)	79.75 (0.06)	41.23 (0.11)	75.77 (0.21)	41.67 (0.03)	80.69 (0.24)	43.43 (0.15)	74.66 (0.05)	38.38 (0.07)
Open-Source Large Vision-Language Models												
DeepSeek-VL2-small [28]	33.16 (0.38)	16.62 (0.11)	36.22 (0.26)	7.89 (0.69)	34.73 (0.35)	12.64 (0.76)	40.23 (0.13)	15.04 (0.67)	39.02 (0.76)	11.89 (0.34)	36.26 (0.36)	12.78 (0.56)
InternVL2-8B [8]	80.60 (0.37)	39.43 (0.67)	81.95 (0.96)	39.01 (0.04)	78.66 (0.75)	38.42 (0.81)	75.55 (0.38)	39.46 (0.18)	75.85 (0.12)	39.25 (0.26)	79.11 (0.18)	39.12 (0.46)
InternVL3-14B [8]	85.27 (0.75)	53.04 (0.23)	82.13 (0.19)	26.10 (0.14)	82.01 (0.64)	48.59 (0.19)	80.65 (0.45)	47.40 (0.17)	79.41 (0.18)	59.41 (0.46)	82.32 (0.37)	44.12 (0.34)
InternVL3.5-8B [8]	75.17 (0.08)	46.95 (0.24)	64.99 (0.18)	26.57 (0.16)	70.43 (0.32)	44.06 (0.37)	66.21 (0.24)	47.04 (0.48)	73.05 (0.23)	49.94 (0.39)	69.04 (0.05)	40.66 (0.47)
Llama-4-Scout [40]	86.19 (0.16)	46.10 (0.44)	84.12 (0.23)	39.95 (0.73)	84.36 (0.21)	43.41 (0.34)	84.59 (0.14)	45.75 (0.03)	81.69 (0.13)	43.41 (0.17)	84.53 (0.28)	43.63 (0.18)
LlAVA-NeXT-13B [26]	29.30 (1.08)	23.89 (9.75)	46.65 (0.76)	27.13 (6.05)	43.79 (0.35)	26.23 (1.98)	33.38 (0.14)	27.24 (0.54)	46.38 (0.17)	26.91 (2.77)	39.11 (0.64)	26.15 (3.99)
Qwen2.5-VL-72B [9]	78.10 (0.91)	38.13 (0.01)	79.55 (0.62)	35.01 (0.97)	74.64 (0.14)	32.78 (0.12)	75.26 (0.67)	34.53 (0.31)	71.49 (0.94)	32.75 (0.17)	76.61 (0.39)	35.05 (0.02)
Qwen3-VL-8B [3]	77.77 (0.17)	42.72 (0.17)	68.83 (0.13)	38.65 (0.05)	80.14 (0.42)	41.31 (0.09)	75.53 (0.02)	43.23 (0.23)	80.46 (0.04)	46.39 (0.43)	74.83 (0.04)	41.17 (0.04)
TinyLLaVA-2B [57]	20.93 (0.13)	2.40 (0.02)	41.91 (0.23)	5.30 (0.00)	28.06 (0.14)	5.93 (0.01)	24.76 (0.34)	3.65 (0.01)	23.39 (0.16)	5.04 (0.05)	28.81 (0.37)	4.34 (0.01)
GLM-4.6V [17]	77.10 (0.19)	43.18 (0.15)	69.89 (0.20)	36.80 (0.14)	79.78 (0.13)	41.67 (0.07)	75.00 (0.09)	44.40 (0.18)	80.45 (0.08)	51.13 (0.23)	74.90 (0.09)	41.09 (0.32)

configurations. In total, we systematically assess 5 proprietary models and 25 open-source models spanning multiple architectural variants.

Our evaluation primarily focuses on zero-shot performance to analyze the intrinsic capabilities of each model without task-specific fine-tuning. All experiments are conducted on servers equipped with NVIDIA A800 GPUs. Detailed information regarding model hyperparameter settings is in the Appendix 3.2.

6.2 Main Results

Accuracy of the Final Answer. We evaluated the final answer accuracy of VLMs on AgroCoT, as shown in Fig. 6 (a). Proprietary models generally outperform open-source models, with GPT-5 leading at over 60% accuracy, followed by Gemini-2.5-Pro and GPT-4.1, both nearing 60%. Among open-source models, Qwen3-VL-8B and InternVL3-14B achieve competitive results with accuracies above 55%. While most models surpass the 45% baseline, none exceeds 70%, highlighting the significant challenge that AgroCoT presents to VLMs in the agricultural domain. Notably, InternVL3.5 shows no improvement over its predecessor, suggesting that current models may not have been optimized with agricultural domain knowledge, and the gaps identified by AgroCoT are not yet a primary focus in mainstream model development.

Semantic Similarity and Key Steps Matching. We evaluated the reasoning generation capabilities of the models based on semantic similarity and key steps matching, as shown in Tab. 2. Semantic similarity measures the proximity between the model’s output and the reference CoT, reflecting its ability to capture shallow semantics. GPT-4.1 outperformed all models with an average similarity score of 88.59, while Llama-4-Scout led the open-source models with a score of 84.53. GPT-4.1 performed best across all dimensions except for OD, where Claude-Sonnet-4.5 was slightly better. Among open-source models, InternVL3-14B and Llama-4-Scout showed comparable results. For key steps matching, the results aligned closely with semantic similarity scores. GPT-4.1 maintained its lead in overall CoT quality. Notably, InternVL3-14B had the

Table 3: Comprehensive performance evaluation of representative VLMs. LLM denotes the LLM-based evaluator (maximum score: 50), while Human represents human evaluation scores on a 1–5 scale. Boldface indicates the best overall performance across all models. Peach and Lemon denote the best and second-best results among open-source models, respectively. Llama-4-Scout denotes Llama-4-Scout-17B-16E-Instruct. All results are reported as mean (standard deviation) over three independent runs.

Model	QA		SU		OD		DM		EM		Overall	
	LLM	Human										
Proprietary Large Vision-Language Models												
Claude-Sonnet-4.5	40.26(1.40)	1.80(0.28)	40.49(1.86)	2.71(0.10)	43.68(1.54)	4.76(0.25)	44.24(1.35)	3.39(0.26)	44.68(1.17)	4.11(0.30)	42.25(1.43)	3.60(0.18)
Gemini-2.5-Pro [39]	41.90(0.81)	2.25(0.07)	43.59(0.88)	3.61(0.25)	45.65(1.24)	4.03(0.21)	47.29(0.22)	3.84(0.15)	47.70(0.31)	4.32(0.30)	44.77(0.56)	3.81(0.22)
GPT-4.1 [1]	39.41(1.40)	2.50(0.57)	40.26(1.61)	3.36(0.30)	43.29(1.84)	4.24(0.33)	45.11(1.27)	3.47(0.15)	45.85(1.12)	4.12(0.38)	42.18(1.34)	3.70(0.33)
GPT-5 [21]	35.17(1.43)	2.60(0.14)	38.08(1.57)	3.46(0.76)	39.70(2.05)	3.94(0.58)	42.08(1.40)	3.47(0.52)	42.40(1.84)	4.00(0.51)	38.89(1.61)	3.63(0.49)
Doubao-Seed-1.8 [35]	35.47(1.85)	2.00(0.47)	36.95(1.41)	3.00(0.35)	44.84(0.21)	4.08(0.35)	46.36(0.42)	3.50(0.71)	47.87(0.47)	4.64(0.51)	40.22(1.22)	3.71(0.24)
Open-Source Large Vision-Language Models												
DeepSeek-VL2-small [28]	7.00(3.59)	1.15(0.07)	10.26(5.16)	1.18(0.05)	18.73(7.54)	1.41(0.08)	16.24(6.71)	1.18(0.04)	16.33(6.45)	1.34(0.03)	12.75(5.65)	1.27(0.02)
InternVL2-8B [8]	31.43(3.63)	1.70(0.14)	33.39(1.54)	2.36(0.20)	37.54(2.54)	2.85(0.46)	36.11(3.82)	2.37(0.22)	37.59(3.65)	2.96(0.45)	34.64(2.94)	2.57(0.33)
InternVL3-14B [8]	35.31(1.98)	2.05(0.07)	36.37(2.80)	2.93(0.20)	39.74(2.55)	4.26(0.12)	39.03(2.59)	3.45(0.04)	41.39(2.28)	3.70(0.08)	37.76(2.45)	3.44(0.10)
InternVL3.5-8B [8]	34.63(1.49)	1.50(0.71)	32.02(3.51)	1.62(0.18)	41.73(2.48)	4.17(0.00)	42.04(2.86)	4.00(0.35)	45.74(2.72)	3.86(0.81)	36.95(2.72)	3.29(0.41)
Llama-4-Scout [40]	35.70(1.82)	1.85(0.07)	33.58(2.54)	3.32(0.25)	37.90(2.31)	3.53(0.50)	40.76(1.87)	3.34(0.11)	41.21(2.08)	4.05(0.33)	37.96(2.10)	3.43(0.27)
LLaVA-NeXT-13B [26]	7.71(2.02)	1.05(0.07)	10.39(1.05)	1.07(0.00)	10.63(2.56)	1.15(0.12)	9.68(1.61)	1.37(0.07)	14.41(2.44)	1.43(0.30)	10.04(1.10)	1.26(0.05)
Qwen2.5-VL-7B [3]	30.13(1.88)	2.15(0.21)	30.27(3.12)	2.46(0.35)	36.78(3.34)	3.44(0.29)	35.28(3.99)	3.26(0.45)	35.18(3.48)	3.43(0.20)	32.93(3.00)	3.10(0.30)
Qwen3-VL-8B [3]	40.82(0.43)	3.83(0.24)	34.94(1.99)	2.88(0.18)	44.05(0.67)	4.00(0.24)	45.89(0.20)	4.62(0.53)	47.19(0.12)	4.14(0.40)	40.38(1.18)	3.94(0.32)
TinyLLaVA-2B [57]	13.07(4.22)	1.60(0.00)	13.08(3.06)	2.14(0.10)	19.84(1.16)	2.53(0.17)	20.11(3.33)	2.37(0.37)	22.44(2.80)	1.93(0.25)	16.65(3.06)	2.14(0.21)
GLM-4.6V [17]	38.54(1.85)	4.00(0.47)	33.97(1.85)	3.75(0.00)	45.25(1.74)	4.00(0.47)	45.15(1.61)	3.38(0.53)	47.85(1.25)	3.93(0.51)	39.82(1.71)	3.83(0.41)

strongest key steps coverage in QA and EM, indicating a higher overlap with the vocabulary of the standard answers in these tasks.

LLM Scoring and Human Evaluation. In the LLM Score evaluation presented in Tab. 3, Gemini-2.5-Pro leads with a score of 44.77, excelling in SU and DM dimensions, though slightly underperforming Doubao-Seed-1.8 in EM. Among open-source models, Qwen3-VL-8B and GLM-4.6V show similar performance, with Qwen3-VL-8B slightly leading overall. InternVL3-14B stands out in the SU dimension, showcasing its potential in spatial understanding for agriculture. Human evaluation results align with LLM scores, with Qwen3-VL-8B ranking highest among open-source models (3.94), followed by GLM-4.6V (3.83). Gemini-2.5-pro leads in closed-source models with 3.81, confirming its strength in deep reasoning. These findings suggest that combining automatic and human evaluation offers a comprehensive view of model performance in complex agricultural reasoning tasks.

Additional results using ROUGE and BERTScore metrics are presented in Appendix 4, while Appendix 6 includes examples highlighting AgroCoT’s integration of visual information and reasoning challenges.

6.3 Discussion

Does model performance scale with the size? Fig. 6 (a) illustrates how the accuracy of models varies with model size on AgroCoT. Although the accuracy of most models improves as the model size increases, there are still some models whose performance actually decrease, such as DeepSeek-VL2 and Qwen2.5-VL. This indicates that increasing the size of the model does not enhance its capabilities in the agricultural domain all the time. In Appendix 5.1, we provide an analysis of how reasoning capabilities change with model size.

Do LLMs and humans share similar evaluation tendencies for reasoning? Using LLMs as automatic evaluators has become common in experimental evaluation, but whether LLM scores truly reflect human reasoning pref-

both answer generation and complex reasoning. Additionally, we introduce multi-dimensional evaluation metrics from four distinct perspectives to establish a systematic evaluation framework. Through the evaluations of 30 models, we find that both proprietary and open-source VLMs encounter significant challenges in agricultural reasoning, without notable improvements observed in version updates. We hope AgroCoT will offer valuable guidance for the development of agriculture-specific models and foster the integration of domain knowledge with reasoning capabilities.

Appendix

Table of Contents

- 1. Data Collection**
 - 1.1 Data Sources Selection
 - 1.2 Data Filtering
 - 1.3 Geospatial Distribution
- 2. CoT Construction Details**
 - 2.1 Prompt Design
 - 2.2 Wrong CoT Filtering
 - 2.3 Human Refinement
- 3. Experiment Details**
 - 3.1 More Evaluation Protocols
 - 3.2 Evaluation Models
 - 3.3 LLM Evaluator
 - 3.4 Human Evaluation
- 4. More Experimental Results**
 - 4.1 Accuracy, ROUGE-L F1 and BERTScore F1 Evaluation
 - 4.2 Keyword Extraction Capability
 - 4.3 Coherence and Fluency of Reasoning Texts
 - 4.4 Semantic Evaluation of Reasoning Content
 - 4.5 Performance at the Second-Level Dimensions
- 5. Further Discussion**
 - 5.1 Does the reasoning ability of VLMs improve as the parameters increase?
 - 5.2 Are VLMs capable of handling deep reasoning tasks?
- 6. Dimension Details and Case Study**
- 7. Limitations and Future Work**
- 8. Ethical Considerations**

1 Data Collection

1.1 Data Sources Selection

AgroCoT is constructed based on four state-of-the-art agricultural vision-language benchmarks (see Tab. 1), each offering unique characteristics and specialized annotations for comprehensive evaluation of VLMs in agriculture.

CDDM [27] enhances our dataset with **large-scale crop disease coverage**, comprising 137,000 disease images and 1 million question-answer pairs spanning 16 crop types and 60 disease categories. The dataset combines web-collected imagery with field survey photographs, ensuring diverse representation of agricultural scenarios. A distinctive aspect is the inclusion of GPT-4 generated instruction-following data with carefully designed negative response examples, addressing the critical challenge of model over-confidence in disease diagnosis.

AGMMU [14] contributes **real-world conversational data** derived from 116,231 authentic dialogues between farmers and USDA-authorized agricultural experts. This dataset uniquely provides both multiple-choice questions (MCQs) and open-ended questions (OEs), with 746 instances of each format, all rigorously verified by human annotators. The accompanying AGBASE development corpus contains 57,079 multimodal facts, facilitating comprehensive model training and evaluation across five critical agricultural knowledge types: insect identification, species recognition, disease categorization, symptom description, and management instruction.

Table 1: More details of data sources used in AgriCoT.

Dataset	Year	Key Features
CDDM [27]	2024	137,000 images of various crop diseases; 1 million question-answer pairs; for the crop and disease categories, detailed disease insights, and prevention and control strategies
AGMMU [14]	2025	746 multiple-choice questions and 746 open-ended questions; from real-world conversations between users and USDA-funded experts; human verification; five major agricultural knowledge types
AgroMind [22]	2025	28,482 QA pairs and 20,850 images; four task dimensions and 13 task types; three sensor types; from nine RS datasets and one proprietary global parcel dataset
AgroBench [37]	2025	4,342 QA pairs, 203 crop categories and 682 disease categories; 98 machine categories and 77 traditional management methods; multiple-choice format; annotated by human agronomist experts

AgroMind [22] serves as the core benchmark in our integrated dataset, providing a **multi-dimensional and multi-scene agricultural remote sensing evaluation framework**. It comprises 28,482 question-answer pairs and 20,850 images sourced from 9 public datasets and 1 private global parcel dataset, spanning diverse agricultural scenarios including pest and disease monitoring, parcel analysis, multiple crop recognition, and anomaly detection. AgroMind uniquely

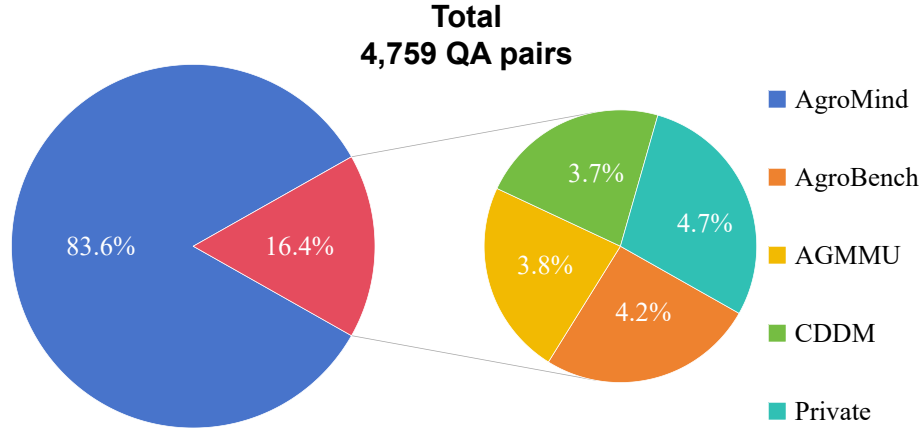


Fig. 1: Percentage of Different Datasets.

covers four hierarchical task dimensions—spatial perception, object understanding, scene understanding, and scene reasoning—with 13 specific task types ranging from basic classification to advanced reasoning. The dataset integrates multi-sensor data from UAVs, satellites, and ground cameras, supporting various question formats including judgment, counting, text choice, image choice, and open-ended questions. A distinctive feature is its logical enhancement strategy in QA pair design, where hierarchical reasoning processes are artificially predefined rather than directly using raw annotations as answers.

AgroBench [37] serves as a foundational component of our dataset, distinguished by its **expert annotations from professional agronomists**. This benchmark covers 7 distinct agricultural tasks including disease identification, pest recognition, weed detection, crop management, disease management, machinery usage, and traditional farming methods. With an extensive coverage of 203 crop categories, 682 disease types, 134 pest species, and 108 weed varieties, it provides 4,342 carefully curated question-answer pairs supported by 3,745 high-quality images captured in real farm environments. A notable feature is the inclusion of bounding box annotations for precise weed localization, enabling fine-grained visual understanding tasks.

1.2 Data Filtering

The datasets from CDDM, AGMMU, AgroMind and AgroBench were carefully selected and filtered to create a more comprehensive and relevant agricultural benchmark for AgroCoT. As shown in Fig. 1, the figure illustrates the proportion of samples contributed by each source dataset. AgroMind, contributing 3,980

question-answer pairs, preserves its strengths by retaining multi-view, multi-scenario, and multi-regional data, ensuring the broad coverage of agricultural tasks. To minimize redundancy and enhance data variety, we extract the most distinctive and valuable data from other sources. Specifically, CDDM contributes 175 question-answer pairs, AGMMU provides 180 pairs, and AgroBench adds 200 pairs. Additionally, we have included 224 self-constructed private data points. This selection process not only maximizes diversity but also ensures that AgroCoT captures the unique advantages of each dataset, resulting in a more robust and expansive benchmark for evaluating models on agricultural tasks. Overall, our integrated dataset synthesizes the complementary strengths of these benchmarks, creating a unified evaluation framework that spans:

- **Multiple agricultural domains:** From fine-grained disease identification to practical management recommendations.
- **Diverse annotation formats:** Including multiple-choice, open-ended, and judgement tasks.
- **Real-world relevance:** Incorporating authentic farmer queries and expert-verified responses.
- **Comprehensive coverage:** Encompassing crops, diseases, pests, weeds, machinery, and traditional practices.
- **Multiview image sources:** Including images captured by remote sensing satellites, low-altitude drone imagery, and ground-based handheld cameras.
- **Multi-dimensional evaluation:** Supporting assessment across object detection, quantitative analysis, disease monitoring, spatial understanding, and environmental management.

This comprehensive integration enables robust assessment of VLMs in addressing practical agricultural challenges while maintaining scientific rigor through expert validation and diverse task formulations.

1.3 Geospatial Distribution

AgroCoT retains substantial geographical diversity even after sampling, ensuring that the dataset continues to represent a wide spectrum of agricultural environments (see Fig. 2). Moreover, the incorporation of additional private datasets further expands the spatial coverage, enriching the diversity of regions and strengthening the global representativeness of AgroCoT.

Specifically, the dataset covers a broad range of climatic and agricultural zones:

- **Climate diversity:** The samples span tropical regions (*e.g.*, Indonesia), temperate zones (*e.g.*, European countries, Japan), and continental climates (*e.g.*, Ukraine, Russia), ensuring representation across major global climate regimes.
- **Land-use variation:** AgroCoT includes data from highly industrialized monoculture systems (such as the U.S. Corn Belt) as well as diverse polyculture farming landscapes (*e.g.*, Tanzania), capturing a wide range of agricultural practices and intensities.

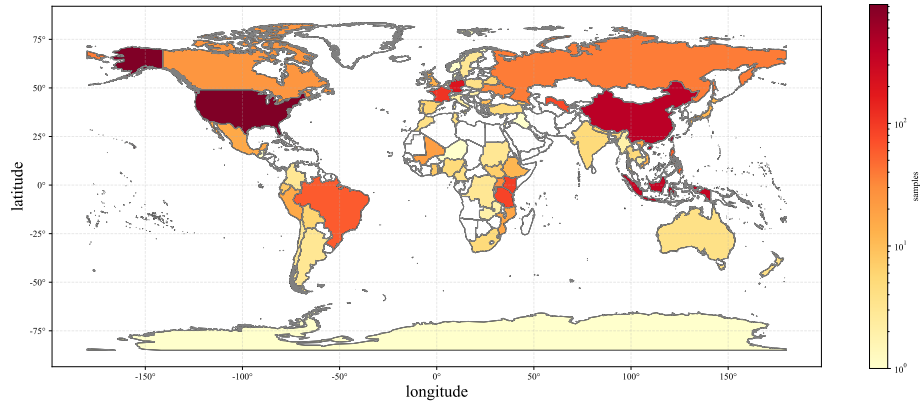


Fig. 2: Worldwide Distribution of AgroCoT.

- **Crop phenology:** The dataset reflects growth cycles of major staple crops including maize, rice, and oil palm, providing coverage across key phenological stages in different agricultural regions.

This rich and globally distributed dataset enables comprehensive cross-regional generalization analysis, supporting research on robust agricultural decision-making and sustainable global crop management.

2 CoT Construction Details

2.1 Prompt Design

To ensure that the CoTs generated by GPT-4o exhibit both deep reasoning and a consistent structure, we design a prompt template (see Fig. 3). In addition to the basic inputs (reference image, question, and options), the template explicitly guides the model to clarify the core problem, produce detailed and coherent visual descriptions, systematically analyse each option, and form a complete reasoning chain from analysis to conclusion. This structured prompting strategy is intended to steer the model through multi-step, in-depth reasoning while maintaining a standardized output format. To ensure fairness and reproducibility in the evaluation process, we used standardized input settings across all comparative experiments. Specifically, for each test sample, we provided all models to be evaluated with the exact same prompt template.

2.2 Wrong CoT Filtering

GPT-4o’s pre-generated answers and reasoning chains frequently exhibit issues such as incorrect conclusions, formatting errors, missing details, shallow reasoning, and logical inconsistencies. To mitigate this, we adopt a rigorous two-stage

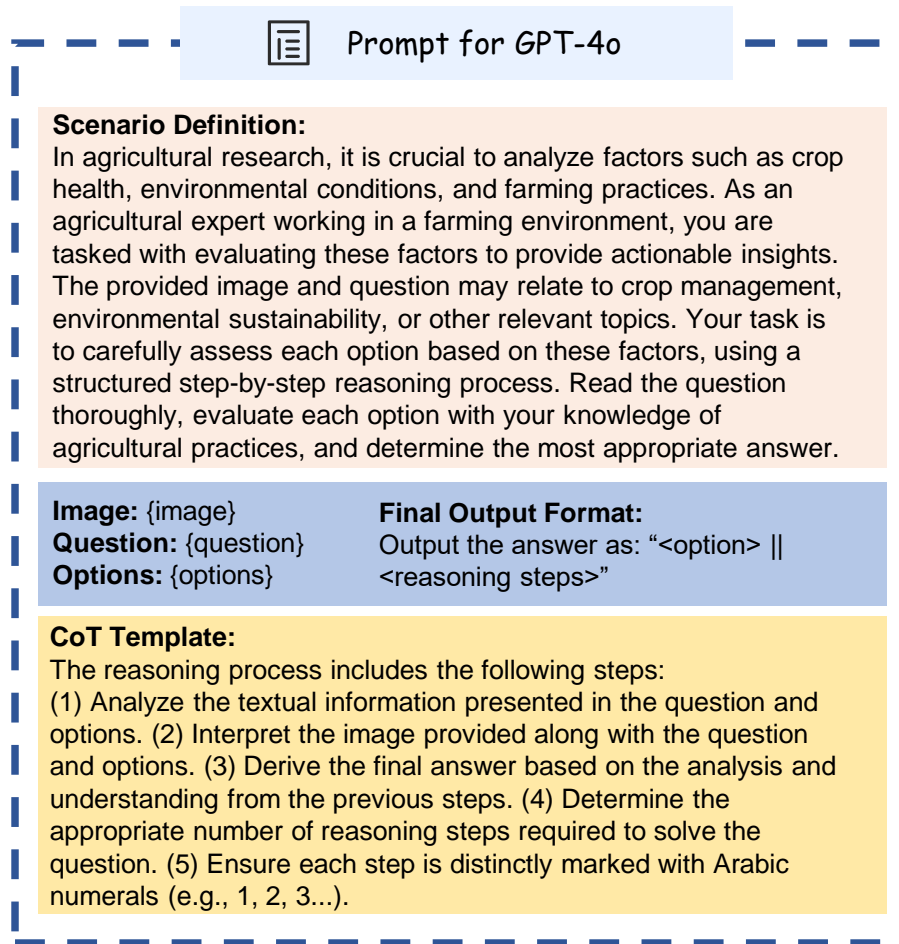


Fig. 3: CoT pre-generation prompt.

screening procedure. First, we discard samples whose final answers are incorrect, as erroneous conclusions usually indicate fundamental flaws in the underlying reasoning. Second, for samples with correct answers, we do not accept them directly; instead, we carefully re-check each chain against criteria on length, formatting, content completeness, and reasoning rigor. This process filters out CoTs that fail to meet our standards of well-structured format, deep reasoning, multi-step derivation, and logical consistency, and flags them for subsequent human refinement.

2.3 Human Refinement

To ensure the quality of CoT construction in AgroCoT, we formed a labeling team of 20 volunteers responsible for writing and refining the reasoning chains. The team consists of 5 undergraduate students and 15 graduate students, all with backgrounds in agricultural science, computer science, or related fields, and they underwent standardized labeling training. Through multiple rounds of manual review and cross-validation, we ensured that each reasoning chain met high-quality standards in terms of logical coherence, domain accuracy, and clarity of expression.

Before beginning the annotation work, they underwent pre-task training and a qualification test to ensure a solid understanding of both the agricultural scenarios and the CoT refinement criteria. During the refinement process, all annotators followed a detailed editing guideline, which specified how to correct errors, enrich missing details, standardize formatting, and upgrade shallow or fragmented reasoning into coherent multi-step chains. Under this protocol, the annotators consistently transformed raw model outputs into CoTs that satisfy our requirements of deep reasoning, logical consistency, and clear, well-structured explanations.

Statistical results indicate that over 70% of the reasoning chains underwent manual editing and content expansion, leading to significant differences between the final version and the original GPT-4o pre-generated reasoning chains. The core objective of this design is to minimize any potential advantage that GPT-series models might gain from data generated by previous versions, ensuring that the evaluation results on the AgroCoT benchmark are fairer and more objective across all models.

3 Experiment Details

3.1 More Evaluation Protocols

We use accuracy as one of the core evaluation metrics, measuring the consistency between the final answer and the standard answer. Given the diverse answer formats in our dataset, we adopt different evaluation strategies tailored to each question type. For multiple-choice and true/false questions, correctness is determined via strict character-level exact matching. For open-ended short responses, we employ a predefined keyword-matching mechanism that allows limited lexical variation while enforcing semantic constraints. For long-form question answering, both model-generated and reference answers are projected into a shared embedding space using a language model, and cosine similarity is computed to quantify semantic alignment.

We supplement the evaluation with ROUGE-1, ROUGE-2, and ROUGE-L, computing precision, recall, and F1 score for each. ROUGE measures n-gram overlap between generated and reference CoTs, reflecting content coverage and sequence structure. Precision indicates how well the model captures relevant

information, while recall shows how comprehensively the model covers the reference. The F1 score balances both metrics. We also use BERTScore to evaluate precision and recall in the embedding space, comparing semantic similarity using cosine similarity of word embeddings. Precision in BERTScore reflects how much of the generated reasoning matches the reference semantically, while recall assesses how well the model captures the reference’s semantic content. F1 score for BERTScore balances both, providing a measure of semantic quality and completeness. These metrics allow for a comprehensive evaluation of both surface-level n-gram overlap and deeper semantic alignment.

3.2 Evaluation Models

As shown in Tab. 2, we evaluate both proprietary and open-source vision-language models that represent the current state of multimodal reasoning. When a model family provides several parameter scales, we include a small and a large variant in order to study the effect of model size on both answer accuracy and CoT quality. Unless otherwise noted, all inputs contain the same images and textual questions, and outputs are requested in the unified “answer then reasoning” format. We use nucleus sampling with temperature=0.1, top-p=0.7 for all models. For models that expose an explicit “thinking mode” switch via API, we enable thinking mode with a fixed configuration (detailed below). For all other decoding parameters, we use the default values recommended by each provider. All local inference for open-source models was run on machines equipped with NVIDIA A800 GPUs, and proprietary models were accessed via their official APIs.

Proprietary Models. We consider five major proprietary multimodal systems accessed through their official APIs: GPT-5 and GPT-4.1 from OpenAI [21], Gemini-2.5-Pro from Google [10], Claude-Sonnet-4.5 from Anthropic, and Doubao-Seed-1.8 from Volcano Engine [35]. All of them support joint image and text input and can produce long-form natural-language responses. For each model we use the recommended chat completion interface with a unified decoding configuration, and we supply a short system instruction that asks the model to first provide the final answer and then provide step-by-step reasoning. We do not apply task-specific fine-tuning, so the reported results reflect the intrinsic zero-shot capabilities of these proprietary models on AgroCoT.

For proprietary models that provide explicit thinking-mode controls, we enable thinking mode with fixed settings: GPT-5 is run with reasoning effort set to medium, Claude-Sonnet-4.5 is run with thinking enabled and budget_tokens=8192, Doubao-Seed-1.8 is run with think-medium. Other proprietary models are queried using their recommended chat completion interfaces under the same sampling configuration, while the models without an explicit thinking-mode switch are used with their default behavior.

DeepSeek-VL2 [28]. DeepSeek-VL2 is an open-source VLM family that integrates a vision encoder with a DeepSeek language backbone for general vision-language understanding. We evaluate three parameter scales, DeepSeek-VL2-tiny (1B parameters), DeepSeek-VL2-small (2.8B), and DeepSeek-VL2 (4.5B).

Table 2: Models grouped by family.

Model Family	Model Name	Year	Parameters
Proprietary, API			
GPT	GPT-5	2025	N/A
	GPT-4.1	2025	N/A
Gemini	Gemini-2.5-Pro	2025	N/A
Claude	Claude-Sonnet-4.5	2025	N/A
Doubao	Doubao-Seed-1.8	2025	N/A
Open-source			
DeepSeek-VL2	DeepSeek-VL2-tiny	2024	1B
	DeepSeek-VL2-small	2024	2.8B
	DeepSeek-VL2	2024	4.5B
InternVL	InternVL2-2B	2024	2B
	InternVL2-4B	2024	4B
	InternVL2-8B	2024	8B
	InternVL2-26B	2024	26B
	InternVL3-2B	2025	2B
	InternVL3-8B	2025	8B
	InternVL3-14B	2025	14B
	InternVL3-38B	2025	38B
	InternVL3.5-38B	2025	38B
LLaVA-NeXT	LLaVA-NeXT-7B-Mistral	2024	7B
	LLaVA-NeXT-8B	2024	8B
	LLaVA-NeXT-13B	2024	13B
	LLaVA-NeXT-34B	2024	34B
Qwen-VL	Qwen2.5-VL-3B-Instruct	2025	3B
	Qwen2.5-VL-7B-Instruct	2025	7B
	Qwen2.5-VL-32B-Instruct	2025	32B
	Qwen3-VL-8B-Instruct	2025	8B
TinyLLaVA	TinyLLaVA-1.5B	2024	1.5B
	TinyLLaVA-2B	2024	2B
	TinyLLaVA-3.1B	2024	3.1B
Meta Llama 4	Llama-4-Scout-17B-16E-Instruct	2025	17B
GLM-V	GLM-4.6V	2025	106B

All checkpoints are loaded from the official HuggingFace releases, and inference follows the evaluation script.

InternVL [8]. The InternVL family couples a high-capacity vision encoder with an InternLM language model and is trained on web-scale image-text data. We evaluate two generations, InternVL2.5 and InternVL3, covering a wide range of model sizes: InternVL2.5-2B, 4B, 8B, 26B and InternVL3-2B, 8B, 14B, 38B. In addition, we run InternVL3.5-38B as a newer high-capacity checkpoint in the series that targets stronger multimodal reasoning. For all InternVL models, we adopt the official OpenGVLab checkpoints and inference implementation without modification, provide each image and question in the recommended chat format, and keep the same unified CoT prompt to elicit natural-language reasoning.

LLaVA-NeXT [26]. LLaVA-NeXT extends the LLaVA framework with updated language backbones and visual instruction tuning. We include four LLaVA-NeXT variants: LLaVA-NeXT-7B-Mistral, 8B, 13B, and 34B. All models are evaluated using the official checkpoints, which pair a CLIP-style vision encoder with different language models.

Qwen-VL [3]. The Qwen-VL family includes both Qwen2.5-VL and Qwen3-VL, covering instruction-tuned vision-language models at multiple parameter scales. We assess three instruction-tuned Qwen2.5-VL variants: Qwen2.5-VL-3B-Instruct, Qwen2.5-VL-7B-Instruct, and Qwen2.5-VL-32B-Instruct. In addition, we evaluate Qwen3-VL-8B-Instruct as a representative model from the newer Qwen3-VL line. All models are loaded from the official Qwen releases, and inference follows the recommended chat template and image preprocessing pipeline.

TinyLLaVA [57]. TinyLLaVA is designed as a lightweight alternative to large VLMs by attaching a compact vision encoder to a small language model, targeting resource-constrained scenarios such as edge devices. We test three publicly available versions, TinyLLaVA-1.5B, 2B, and 3.1B, obtained from the official project page.

Llama-4-Scout [40]. We include Llama-4-Scout-17B-16E-Instruct as a recent large-scale open-source model with strong general reasoning ability. The Scout variant is a natively multimodal model that processes text and images via an integrated vision encoder and projection module in the official implementation.

GLM-V [17]. GLM-V is a family of multimodal models released by Z.ai that targets strong multimodal reasoning and long-context visual understanding. We evaluate GLM-4.6V (106B parameters) using the official checkpoint. We enable its thinking mode during inference, while keeping the same unified CoT prompt and the same sampling configuration (temperature=0.1, top-p=0.7) as in other models.

3.3 LLM Evaluator

To enable the automated and standardized evaluation of model-generated reasoning chains, we designed a structured prompt template, as shown in Fig. 4. The prompt specifies:

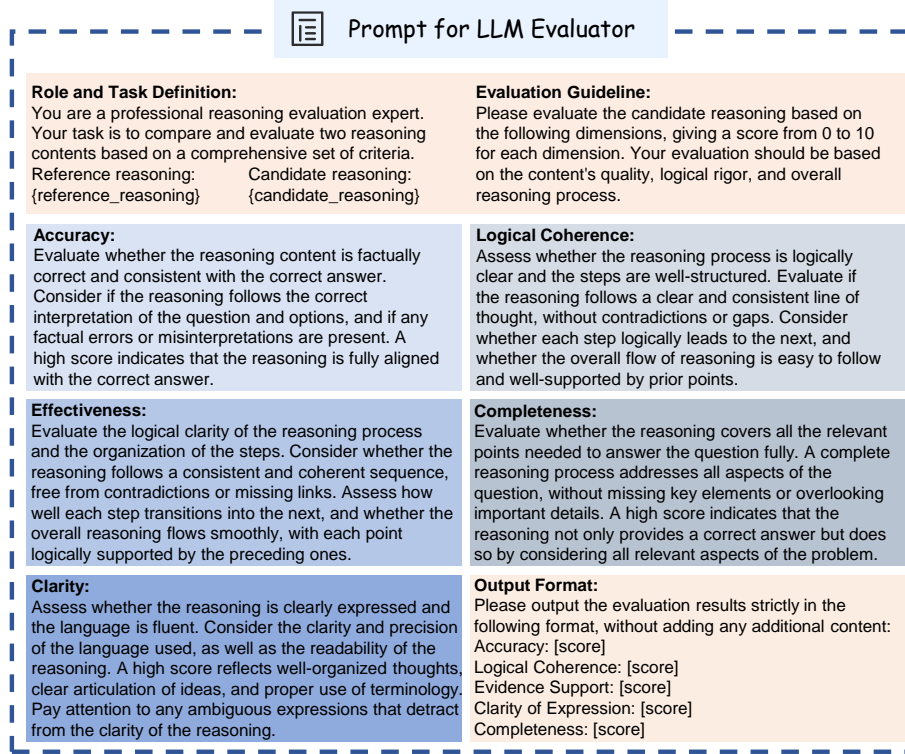


Fig. 4: LLM Scoring prompt.

- **Role and task definition:** The large language model acts as a professional evaluator, tasked with objectively scoring the reasoning chain across multiple dimensions.
- **Evaluation content:** The subject of evaluation is the reasoning chain output generated by the model.
- **Five evaluation dimensions and scoring criteria:** These include accuracy, logical coherence, effectiveness, clarity, and completeness, with detailed scoring guidelines for each dimension.
- **Scoring system:** Each dimension is scored out of 10 points, with a total score of 50 points.
- **Output format requirements:** The model is required to output the scores in a structured format, facilitating automated extraction and statistical analysis.

Through this standardized prompt design, we ensure that each evaluation adheres to a consistent set of standards, while also enabling the automated parsing of dimension scores and the total score from the model's output.

To ensure the reproducibility and cost-effectiveness of the automatic scoring process, we selected open-source large language models as evaluators, all of which

were obtained from the Hugging Face Hub and deployed locally using vLLM. The specific models used include: Qwen/Qwen3-8B, deepseek-ai/DeepSeek-R1-Distill-Qwen-7B, and zai-org/GLM-Z1-9B-0414. The generation parameters for each model are as follows:

- Qwen3-8B: `enable_thinking=True`, `temperature=0.6`, `max_tokens=2048`, `top_p=0.95`, `top_k=20`, `min_p=0`.
- DeepSeek-R1-Distill-Qwen-7B: `temperature=0.6`, `max_tokens=2048`, `top_p=0.95`.
- GLM-Z1-9B-0414: `temperature=0.6`, `max_tokens=2048`, `top_p=0.95`, `top_k=40`.

These parameter settings are designed to balance the diversity and stability of the generated results while ensuring the efficiency and reproducibility of the scoring process.

3.4 Human Evaluation

To ensure consistency between human evaluations and the refinement of reasoning chains, we invited the same 20 volunteers described in Sec. 2.3 to participate in the manual scoring process. The evaluation criteria follow the five dimensions set in Fig. 4. However, to avoid difficulties caused by a large score range, we adjusted the total score from the original 50-point scale to a 5-point scale, distinguishing it from the automatic scores generated by the LLMs. Finally, we calculated the mean and standard deviation of the scores from all volunteers, which served as the results for the human evaluation experiment.

4 More Experimental Results

4.1 Accuracy, ROUGE-L F1 and BERTScore F1 Evaluation

As shown in Tab. 3, proprietary models generally outperform their open-source counterparts in overall accuracy, reflecting their direct question-answering capabilities. GPT-5 achieves the highest accuracy, surpassing Gemini-2.5-pro by 4.38%, with significant improvements in QA, SU, and DM. InternVL3-38B leads in Object Detection, while Gemini-2.5-pro excels in EU. Among open-source models, the InternVL3 family and Llama-4-Scout stand out as strong performers. Notably, Qwen2.5-VL performs well at 3B and 7B scales but experiences a sharp decline at 32B. Across dimensions, most models notably lag in QA and SU, highlighting the challenges in precision computation and spatial reasoning.

ROUGE-L-f and BERTScore-f assess the reasoning capabilities of models through rule-based and semantic matching, respectively. GPT-4.1 achieves the best overall performance on both metrics, particularly excelling in the Quantitative Analysis dimension. In contrast, despite its high accuracy, GPT-5 demonstrates notably weaker reasoning ability than several other models, including some open-source ones. Although the DeepSeek-VL and TinyLLaVA series show

Table 3: Comprehensive performance evaluation of various VLMs. Acc for **Accuracy (%)**; R-L-f for **ROUGE-L F1 (%)**; B-f for **BERTScore F1 (%)**. “-” indicates that the model is unable to output a normal CoT reasoning, resulting in a negative BERTScore. **Boldface** indicates the best overall across all models. **Peach** and **Lemon** denote the best and the second-best among open-source models, respectively.

Model	QA			SU			OD			DM			EM			Overall		
	Acc	R-L-f	B-f															
Proprietary Large Vision-Language Models																		
Claude-Sonnet-4.5	44.22	47.09	48.44	45.20	41.70	43.89	66.34	45.22	45.85	65.82	45.95	45.35	70.09	44.77	44.15	55.83	44.92	45.74
Gemini-2.5-pro [39]	42.72	36.39	35.41	49.64	32.65	30.95	66.99	35.16	32.26	71.11	36.77	33.02	84.15	36.21	32.28	59.14	35.27	32.88
GPT-4.1 [1]	41.75	50.99	52.11	49.02	45.93	48.43	69.38	47.25	48.28	72.11	49.79	49.11	79.46	46.62	45.66	58.96	48.31	49.18
GPT-5 [21]	50.66	30.46	30.42	54.26	27.65	29.55	70.03	27.76	26.21	76.51	29.27	27.92	79.68	28.46	28.83	63.52	28.78	28.69
Open-Source Large Vision-Language Models																		
DeepSeek-VL2 [28]	27.62	16.18	-	15.18	8.63	-	20.41	11.92	-	19.51	11.09	-	28.79	6.52	-	21.56	11.47	-
DeepSeek-VL2-small [28]	34.59	16.92	-	16.34	7.87	-	30.61	12.31	-	27.67	14.86	-	30.13	11.93	-	27.43	12.83	-
DeepSeek-VL2-tiny [28]	18.01	16.79	7.81	15.89	7.24	-	23.56	12.55	-	27.34	10.38	-	32.14	5.42	-	21.87	11.15	-
InternVL2-2B [8]	36.80	29.02	25.68	16.78	28.64	25.52	29.21	29.68	24.49	29.20	29.02	23.78	32.14	27.89	20.07	28.31	28.95	24.46
InternVL2-4B [8]	22.86	40.25	39.35	23.09	34.98	34.63	36.59	33.95	30.67	40.13	36.71	34.07	42.41	34.62	31.66	31.09	36.40	34.60
InternVL2-8B [8]	38.04	38.08	38.72	39.96	38.67	38.04	55.37	37.03	36.41	48.51	38.45	35.95	50.89	38.35	35.80	45.40	38.11	37.24
InternVL2-26B [8]	42.81	38.62	38.74	37.21	40.49	41.24	55.70	37.72	35.52	55.46	38.81	37.43	67.41	37.47	35.73	49.00	38.82	38.15
InternVL3-2B [8]	34.77	39.73	37.54	33.84	33.70	25.88	41.59	34.62	26.21	30.65	34.72	28.25	43.75	37.04	30.67	35.99	35.93	29.81
InternVL3-8B [8]	35.48	42.63	35.05	40.76	39.19	27.60	63.08	38.81	30.94	56.01	39.46	28.35	58.26	40.71	28.83	48.75	40.18	30.41
InternVL3-14B [8]	48.72	46.23	38.44	44.67	38.08	27.34	62.32	42.01	34.51	63.84	40.98	33.71	69.64	40.82	32.86	55.57	41.77	33.39
InternVL3-38B [8]	46.69	44.29	40.51	45.74	38.50	36.89	72.64	39.15	36.50	66.48	39.17	35.17	71.43	38.95	35.34	58.13	40.25	37.22
Llama-4-Scout-17B-16E-Instruct [40]	40.69	44.90	43.63	40.05	37.88	36.87	61.78	41.35	40.31	65.05	43.40	41.18	64.73	41.34	38.65	52.06	41.78	40.29
LLaVA-NeXT-7B-Mistral [26]	27.54	32.36	29.52	14.56	31.89	27.74	22.58	30.79	24.81	24.81	32.87	27.85	39.29	31.05	28.29	23.93	31.90	27.67
LLaVA-NeXT-8B [26]	38.57	34.56	34.54	23.53	37.15	35.48	35.72	34.05	29.77	41.35	35.91	33.81	38.39	33.81	30.99	34.80	35.29	33.31
LLaVA-NeXT-13B [26]	10.06	23.45	10.55	13.85	26.92	19.86	12.05	25.79	17.14	15.21	26.95	16.62	17.86	25.99	17.45	13.21	25.74	16.09
LLaVA-NeXT-34B [26]	49.60	32.13	26.42	29.48	34.04	32.48	50.71	33.12	31.82	39.03	33.19	29.76	46.65	33.98	32.24	42.43	33.20	30.27
Qwen2.5-VL-3B-Instruct [3]	33.27	32.45	31.65	38.28	30.70	27.49	61.45	29.54	24.75	57.33	29.66	24.43	50.00	31.80	26.16	46.70	30.80	27.23
Qwen2.5-VL-7B-Instruct [3]	38.75	36.28	34.09	35.70	33.38	30.63	63.08	31.89	25.82	57.99	32.91	26.76	52.68	31.30	25.94	48.16	35.50	29.28
Qwen2.5-VL-32B-Instruct [3]	33.80	36.73	33.13	15.28	33.33	30.11	16.07	33.85	28.36	17.42	35.05	27.62	23.21	36.11	30.38	21.28	34.90	29.54
TinyLLaVA-1.5B [57]	19.51	18.29	9.28	14.56	7.72	-	17.59	11.16	-	25.58	8.60	-	21.21	10.32	-	19.27	11.49	-
TinyLLaVA-2B [57]	34.51	3.52	-	22.82	5.71	-	45.17	5.28	-	46.64	3.46	-	41.07	4.85	-	36.85	4.54	-
TinyLLaVA-3.1B [57]	33.45	16.06	4.76	18.12	12.65	0.93	41.91	11.58	-	40.35	10.40	-	48.66	13.51	2.41	34.24	12.92	0.37

low ROUGE scores, this does not necessarily imply reliable reasoning; their consistently low BERTScores indicate incoherent reasoning outputs and poor semantic alignment. Among open-source models, the InternVL2, InternVL3, and Llama-4-Scout series exhibit the strongest reasoning capabilities, outperforming both Gemini-2.5-pro and GPT-5 by a significant margin.

4.2 Keyword Extraction Capability

The ROUGE-1 scores presented in Tab. 4 provide insights into the reasoning capabilities of the evaluated models across various tasks. ROUGE-1, which measures the overlap of unigrams between the generated CoT and the reference, reflects the model’s ability to generate keywords in reasoning texts. Across all tasks, proprietary models like Gemini-2.5-pro and GPT-4.1 perform exceptionally well in recall and F1 score, indicating their strong ability to retain key word in the reasoning process. InternVL2-26B achieves the highest overall precision score, indicating that it generates fewer but more accurate keywords compared to other models. However, the scores of these models across different task types showed minimal variation, suggesting that the models demonstrate consistent keyword reasoning capabilities across all task categories. With the exception of Gemini-2.5-pro, nearly all other models exhibit lower recall compared to precision. This suggests that while the models generate accurate reasoning in certain sections, as reflected in their high precision, there are gaps in the depth of reasoning across longer texts, leading to missed or incomplete coverage when compared to the reference text.

Table 4: Additional performance evaluation of VLMs using **ROUGE-1: Precision, Recall, and F1 Score**. **Boldface** indicates the best overall across all models. **Peach** and **Lemon** denote the best and the second-best among open-source models, respectively.

Model	QA			SU			OD			DM			EM			Overall		
	Precision	Recall	F1															
Proprietary Large Vision-Language Models																		
Claude-Sonnet-4.5	49.18	52.21	50.00	44.56	46.27	44.71	49.38	48.84	48.45	50.85	48.38	49.04	49.96	46.91	47.81	48.48	48.76	47.96
Gemini-2.5-pro [39]	30.76	53.70	38.58	27.40	49.90	34.85	30.61	50.47	37.70	32.34	51.80	39.34	32.39	50.36	38.98	30.37	51.39	37.67
GPT-4.1 [1]	55.93	52.91	53.71	53.82	46.37	49.27	56.93	46.33	50.39	60.48	47.82	52.82	57.65	44.67	49.69	56.69	48.12	51.36
GPT-5 [21]	50.64	25.09	32.79	47.20	22.96	29.99	50.01	22.07	50.14	52.00	22.97	31.52	54.19	21.85	30.64	50.40	23.05	31.09
Open-Source Large Vision-Language Models																		
DeepSeek-VL2 [28]	43.50	11.44	16.61	24.93	6.65	9.10	37.72	10.10	12.75	53.34	9.57	11.65	48.14	4.47	6.81	40.14	8.94	11.99
DeepSeek-VL2-small [28]	49.92	12.08	17.61	35.91	5.38	8.26	48.34	9.39	13.06	46.11	11.21	15.77	50.61	8.45	12.52	45.42	9.34	13.49
DeepSeek-VL2-tiny [28]	48.17	11.81	17.59	30.25	6.04	7.91	45.47	10.02	13.68	56.96	8.51	11.11	62.15	4.31	5.89	46.31	8.61	11.94
InternVL2-2B [8]	57.98	23.44	30.91	47.11	24.82	30.90	56.98	23.25	31.74	55.28	23.42	31.15	53.08	22.91	29.70	54.05	23.69	31.00
InternVL2-4B [8]	55.54	36.25	42.72	55.53	29.95	37.57	54.96	28.93	36.70	57.46	31.35	39.52	55.61	29.02	37.22	55.81	31.50	39.04
InternVL2-8B [8]	60.50	31.78	40.43	54.15	34.82	41.32	55.33	32.08	39.68	57.88	32.75	41.11	55.79	32.89	40.53	56.88	32.90	40.65
InternVL2-26B [8]	61.79	31.56	40.60	60.26	33.99	42.67	62.04	30.80	40.03	62.90	31.41	41.06	63.52	29.66	39.67	61.85	31.79	40.99
InternVL2-72B [8]	55.09	35.11	41.79	52.14	28.99	35.72	54.76	29.33	37.19	56.89	28.45	36.73	55.66	31.67	39.30	54.71	30.74	38.09
InternVL3-8B [8]	56.12	38.98	45.11	51.79	35.89	41.51	54.79	34.80	41.61	55.91	34.83	42.10	56.02	36.20	43.28	54.72	36.26	42.72
InternVL3-14B [8]	57.92	43.65	48.78	53.03	34.10	40.55	57.01	38.09	45.00	57.03	36.45	43.78	55.70	36.96	43.61	56.12	38.05	44.46
InternVL3-30B [8]	62.27	38.40	46.60	54.76	33.83	41.15	56.68	33.93	41.83	57.36	33.75	41.88	57.55	33.53	41.74	57.82	34.95	42.85
Llama-4-Scout-17B-16E-Instruct [40]	46.79	51.42	47.52	38.98	46.64	40.62	41.54	50.28	44.50	46.44	48.65	46.70	45.28	45.87	44.44	43.57	48.90	44.73
LLaVA-NeXT-TB-Mistral [26]	62.04	25.87	34.84	59.74	24.63	33.82	57.74	24.55	33.25	59.33	25.89	35.37	61.58	23.06	32.77	60.01	25.02	34.16
LLaVA-NeXT-8B [26]	56.37	29.06	36.47	61.49	28.71	38.53	62.59	26.05	36.18	60.40	28.74	38.06	59.29	26.18	35.85	59.99	28.01	37.18
LLaVA-NeXT-13B [26]	35.86	20.71	25.31	44.28	22.04	28.92	50.02	20.97	27.54	43.29	22.34	28.39	46.32	20.75	27.72	43.34	21.42	27.51
LLaVA-NeXT-34B [26]	49.79	27.24	34.42	62.73	25.75	35.89	58.26	26.25	35.50	61.11	25.79	35.42	59.85	25.98	35.74	57.98	26.25	35.33
Qwen2.5-VL-72B-Instruct [3]	53.68	26.48	34.41	43.91	29.11	33.37	52.56	24.40	32.37	49.69	25.15	32.52	48.57	28.53	34.64	49.72	26.65	33.38
Qwen2.5-VL-72B-Instruct [3]	54.11	31.67	38.71	48.49	32.17	36.35	54.23	27.49	34.94	54.12	28.05	35.96	56.40	26.58	33.94	52.97	29.72	36.34
Qwen2.5-VL-32B-Instruct [3]	40.35	44.97	39.47	32.96	40.88	35.69	35.94	41.24	36.50	36.26	43.72	37.52	36.96	42.28	38.54	36.46	42.68	37.45
TinyLLaVA-1.5B [57]	72.82	11.27	18.88	41.17	5.01	7.89	56.20	7.40	11.65	55.21	5.14	8.85	63.05	6.08	10.53	57.10	7.19	11.85
TinyLLaVA-2B [57]	38.74	2.08	3.57	33.76	3.52	5.96	38.47	3.52	5.76	36.69	2.06	3.57	64.23	2.81	5.07	39.56	2.80	4.75
TinyLLaVA-3.1B [57]	61.30	10.70	16.62	48.52	8.58	13.02	48.00	7.62	12.04	50.28	6.50	10.77	60.55	8.51	13.94	53.15	8.49	13.36

4.3 Coherence and Fluency of Reasoning Texts

ROUGE-2 primarily evaluates the overlap of bigrams between the model’s generated reasoning and the reference, which is closely tied to the coherence and fluency of the reasoning text. A higher ROUGE-2 score indicates better alignment with the reference in terms of more complex word pairings, reflecting the model’s ability to maintain coherent and logical connections in its reasoning steps. Compared to ROUGE-1 in Tab. 4, all ROUGE-2 scores show a noticeable decline, indicating that all models exhibit gaps in reasoning fluency, particularly in terms of maintaining coherent and logically connected reasoning chains. As illustrated in Tab. 5, GPT-4.1 exhibits the highest ROUGE-2 scores across most tasks, particularly in DM and EM. This suggests that GPT-4.1 generates more fluent and coherent reasoning chains, with well-structured and logically connected word pairs. Its higher ROUGE-2 scores indicate that reasoning chains tend to follow a more natural flow, with fewer fragmented parts. In contrast, TinyLLaVA-2B shows lower ROUGE-2 scores, indicating that the reasoning produced by it may be less fluent, with poorer coherence between consecutive terms in the generated text. These models with low ROUGE-2 scores appear to generate reasoning chains that lack depth and fluency, often resulting in disjointed or incomplete logical connections.

Tab. 6 complements the ROUGE-L scores by providing a comprehensive evaluation of the models’ keyword coverage and reasoning fluency. Gemini-2.5-pro achieves the highest recall rate, indicating its superior ability to capture and reason with complex information. In contrast, InternVL2-26B demonstrates the best precision rate, reflecting its high accuracy in handling smaller, more focused reasoning tasks.

Table 5: Additional performance evaluation of VLMs using **ROUGE-2: Precision, Recall, and F1 Score**. **Boldface** indicates the best overall across all models. **Peach** and **Lemon** denote the best and the second-best among open-source models, respectively.

Model	QA			SU			OD			DM			EM			Overall		
	Precision	Recall	F1															
Proprietary Large Vision-Language Models																		
Claude-Sonnet-4.5	24.64	26.11	24.94	19.37	19.67	19.11	22.89	22.20	22.13	22.91	21.17	21.68	22.19	19.76	20.54	22.39	21.10	21.83
Gemini-2.5-pro [39]	11.85	23.31	15.45	9.13	18.51	11.99	11.19	20.22	14.20	11.73	20.22	14.62	11.78	19.31	14.40	11.01	20.48	14.07
GPT-4.1 [1]	31.23	29.40	29.80	28.24	23.13	25.05	31.12	24.14	26.65	34.49	25.80	29.03	30.23	21.64	24.74	31.02	25.29	27.33
GPT-5 [21]	15.39	6.26	8.64	14.55	5.54	7.91	14.50	5.14	7.44	15.58	5.38	7.85	18.59	5.60	8.43	15.35	5.61	8.04
Open-Source Large Vision-Language Models																		
DeepSeek-VL2 [28]	15.79	4.68	6.78	5.73	2.40	3.17	8.71	3.50	4.23	7.79	3.36	3.93	11.75	1.32	1.88	9.86	3.28	4.31
DeepSeek-VL2-small [28]	11.48	3.86	5.43	6.58	1.62	2.37	13.82	2.85	3.91	12.16	3.52	4.86	20.39	2.63	3.89	11.75	2.91	4.09
DeepSeek-VL2-tiny [28]	21.58	4.54	7.09	8.74	1.89	2.51	10.24	2.76	3.96	11.98	2.35	3.15	2.24	1.03	1.33	12.26	2.73	3.96
InternVL2-2B [8]	26.95	10.45	13.51	18.05	9.33	11.47	21.91	7.65	10.71	23.17	8.58	11.57	19.79	8.34	10.86	22.25	9.02	11.78
InternVL2-4B [8]	26.19	16.84	19.75	23.61	12.13	15.23	21.58	10.90	13.83	23.37	12.32	15.55	22.87	11.20	14.49	23.72	13.00	16.07
InternVL2-8B [8]	28.03	13.79	17.72	22.72	14.37	16.96	22.41	12.47	15.54	24.29	12.91	16.44	24.44	13.47	16.86	24.44	13.46	16.75
InternVL2-26B [8]	29.72	14.70	19.05	28.24	15.22	19.31	26.70	12.52	16.42	28.91	13.45	17.87	29.61	12.44	17.04	28.57	13.91	18.15
InternVL2-38B [8]	23.56	14.47	17.37	21.24	11.28	13.88	20.13	10.06	12.92	21.70	9.90	13.01	22.37	12.29	15.27	21.80	11.65	14.52
InternVL3-8B [8]	25.12	16.97	19.67	22.22	14.90	17.32	21.70	13.35	16.05	22.91	13.54	16.60	25.00	14.93	18.28	23.25	14.83	17.60
InternVL3-14B [8]	29.03	21.43	23.97	22.49	14.00	16.78	25.22	16.35	19.45	25.07	14.96	18.36	25.24	15.79	18.83	25.46	16.70	19.64
InternVL3-38B [8]	30.26	17.61	21.73	23.12	13.44	16.66	23.61	12.94	16.40	24.21	12.88	16.48	25.18	13.03	16.82	25.42	14.23	17.85
Llama-4-Scout-17B-16E-Instruct [40]	22.82	25.52	23.09	15.94	20.52	17.00	17.67	22.48	19.24	19.71	21.29	20.00	18.81	19.53	18.57	19.05	22.22	19.73
LLaVA-NeXT-7B-Mistral [26]	26.88	10.83	14.77	27.44	10.19	14.25	22.79	8.72	12.05	21.74	8.62	12.01	26.11	8.65	12.61	25.08	9.58	13.32
LLaVA-NeXT-8B [26]	26.34	13.76	17.09	29.36	12.92	17.62	26.44	10.09	14.24	25.03	11.08	14.91	26.05	10.08	14.27	26.82	11.91	15.93
LLaVA-NeXT-13B [26]	9.21	4.84	6.00	14.61	7.13	9.41	13.16	5.64	7.46	13.41	6.72	8.50	15.73	6.06	8.42	12.84	6.07	7.88
LLaVA-NeXT-34B [26]	19.98	9.73	12.64	28.72	11.01	15.54	22.86	9.18	12.81	22.20	8.62	12.06	25.02	9.78	13.79	23.68	9.72	13.39
Qwen2.5-VL-3B-Instruct [3]	25.87	11.73	15.64	17.71	10.79	12.54	20.30	7.90	10.90	19.61	8.66	11.63	20.13	10.37	13.03	20.90	9.95	12.85
Qwen2.5-VL-7B-Instruct [3]	27.13	14.58	18.20	21.17	13.11	14.84	20.89	9.46	12.26	23.01	10.46	13.86	26.58	10.49	13.81	23.51	11.95	14.86
Qwen2.5-VL-32B-Instruct [3]	16.15	19.16	15.95	13.10	16.56	14.15	13.69	16.58	14.19	13.05	16.64	13.80	14.69	16.61	15.10	14.13	17.23	14.63
TinyLLaVA-1.5B [57]	34.19	4.42	7.64	14.42	1.48	2.30	31.62	2.96	4.85	25.20	1.63	2.90	33.64	2.07	3.67	26.90	2.60	4.41
TinyLLaVA-2B [57]	5.29	0.54	0.89	14.30	1.11	1.92	15.21	1.31	2.25	11.05	0.64	1.15	11.58	0.88	1.62	11.32	0.89	1.55
TinyLLaVA-3.1B [57]	21.94	3.67	5.81	17.01	2.53	3.90	18.68	2.12	3.45	18.76	1.81	3.08	26.40	2.80	4.72	19.86	2.61	4.20

4.4 Semantic Evaluation of Reasoning Content

Tab. 7 illustrates the reasoning capabilities of the models from the perspective of semantic similarity in their reasoning text. As it directly measures the semantic alignment between the generated reasoning and the reference, BERTScore provides insight into how well the model captures the underlying meaning, even when the specific wording may differ. GPT-4.1 shows strong precision and recall across multiple tasks, reflecting its ability to generate reasoning chains that are both semantically aligned with the reference and provide a detailed analysis. Claude-Sonnet-4.5 has highest recall in OD and EM with greater depth of reasoning ability. In open-source models, Llama-4-Scout-17B-16E-Instruct has the highest recall and InternVL2-26B has the highest precision.

4.5 Performance at the Second-level Dimensions

Tab. 8 presents the performance of various VLMs across multiple second-level tasks in agricultural scenarios. Among the proprietary models, GPT-5 achieves highest accuracy in SU and DM of first-level dimensions, demonstrating strong performance in tasks requiring fine-grained analysis. Gemini-2.5-pro also performs well, especially in AM and MD, demonstrating a wealth of agricultural management and decision-making knowledge. Among open-source models, InternVL3 series, Llama-4-Scout-17B-16E-Instruct and LLaVA-NeXT-7B-Mistral stand out, with InternVL3-38B excelling in multiple dimensions like OC and PM, while LLaVA-NeXT-7B-Mistral performs well in RC. TinyLLaVA-1.5B show lower accuracy, especially in tasks like SR and PR, suggesting that smaller models may struggle with more complex tasks. The overall trends indicate that proprietary models tend to perform better across multiple second-level tasks,

Table 6: Additional performance evaluation of VLMs using **ROUGE-L: Precision and Recall**. **Boldface** indicates the best overall across all models. **Peach** and **Lemon** denote the best and the second-best among open-source models, respectively.

Model	QA		SU		OD		DM		EM		Overall	
	Precision	Recall										
Proprietary Large Vision-Language Models												
Claude-Sonnet-4.5	46.28	49.20	41.58	43.16	46.07	45.61	47.65	45.33	46.77	43.93	45.39	45.68
Gemini-2.5-pro [39]	29.01	50.65	25.68	46.72	28.54	47.07	30.22	48.43	30.08	46.82	28.43	48.13
GPT-4.1 [1]	53.09	50.25	50.18	43.23	53.35	43.47	56.97	45.12	54.06	41.94	53.29	45.28
GPT-5 [21]	47.11	23.32	43.61	20.62	46.09	20.34	48.88	21.32	50.49	20.27	46.72	21.34
Open-Source Large Vision-Language Models												
DeepSeek-VL2 [28]	42.72	11.13	24.15	6.30	36.55	9.47	52.57	9.09	47.66	4.48	39.32	8.53
DeepSeek-VL2-small [28]	48.79	11.55	35.08	5.12	46.99	8.84	44.35	10.55	49.28	8.03	44.18	8.86
DeepSeek-VL2-tiny [28]	46.43	11.25	29.24	5.45	43.35	9.20	55.58	7.92	61.51	3.93	44.85	8.00
InternVL2-2B [8]	54.61	22.01	43.77	23.01	53.37	21.74	51.75	21.80	50.29	21.50	50.67	22.11
InternVL2-4B [8]	52.32	34.17	51.91	27.86	50.69	26.78	53.33	29.13	51.79	26.97	52.04	29.38
InternVL2-8B [8]	57.07	29.92	50.72	32.58	51.62	29.94	54.09	30.65	52.77	31.14	53.36	30.85
InternVL2-26B [8]	58.87	30.01	57.27	32.23	58.38	29.04	59.42	29.70	60.08	28.00	58.60	30.10
InternVL3-2B [8]	52.43	33.38	49.37	27.31	51.03	27.29	53.84	26.88	52.55	29.83	51.68	28.99
InternVL3-8B [8]	53.05	36.86	48.95	33.86	51.04	32.48	52.40	32.64	52.69	34.04	51.46	34.10
InternVL3-14B [8]	54.87	41.40	49.88	31.99	53.15	35.59	53.36	34.13	52.10	34.63	52.71	35.76
InternVL3-38B [8]	59.20	36.50	51.28	31.63	53.01	31.76	53.63	31.57	53.73	31.28	54.32	32.83
Llama-4-Scout-17B-16E-Instruct [40]	44.25	48.54	36.34	43.48	38.58	46.76	43.17	45.19	42.13	42.69	40.71	45.68
LLaVA-NeXT-7B-Mistral [26]	57.25	24.09	56.55	23.19	53.37	22.75	55.33	24.03	58.37	21.84	56.01	23.36
LLaVA-NeXT-8B [26]	52.46	27.65	59.28	27.68	58.87	24.52	57.08	27.09	55.97	24.69	56.73	26.62
LLaVA-NeXT-13B [26]	33.40	19.12	41.30	20.49	47.24	19.63	41.13	21.22	43.49	19.46	40.71	20.02
LLaVA-NeXT-34B [26]	46.64	25.39	59.55	24.42	54.51	24.46	57.40	24.13	56.93	24.70	54.61	24.64
Qwen2.5-VL-3B-Instruct [3]	50.75	24.94	40.45	26.78	47.97	22.27	45.38	22.93	44.52	26.24	45.94	24.58
Qwen2.5-VL-7B-Instruct [3]	50.94	29.64	44.56	29.58	49.50	25.13	49.51	25.68	52.46	24.50	48.93	27.41
Qwen2.5-VL-32B-Instruct [3]	37.64	41.91	30.84	38.14	33.27	38.32	33.87	40.89	34.61	39.62	34.01	39.81
TinyLLaVA-1.5B [57]	70.75	10.91	40.74	4.89	54.96	7.03	54.20	4.98	62.18	5.96	55.94	6.95
TinyLLaVA-2B [57]	38.54	2.05	32.93	3.37	37.32	3.21	36.32	1.98	63.36	2.69	38.91	2.66
TinyLLaVA-3.1B [57]	59.75	10.34	47.46	8.33	46.53	7.33	48.97	6.25	59.22	8.24	51.81	8.21

particularly in tasks requiring complex spatial analysis, such as BA, AE and SR.

As presented in Tab. 9 and Tab. 10, ROUGE-L F1 and BERTScore F1 assess the reasoning capability of models across secondary dimensions, with one focusing on content-structural alignment and the other on semantic similarity. As shown in this two tables, the proprietary models, including Claude-Sonnet-4.5 and GPT-4.1, outperform the open-source models across most second-level dimensions. However, several open-source models such as InternVL3 series and Llama-4-Scout-17B-16E-Instruct also exhibit comparable performance in RC, AD and MD.

5 Further Discussion

5.1 Does the reasoning ability of VLMs improve as the parameters increase?

As shown in Fig. 5 (a) and (b), except for InternVL2&3 and Qwen2.5-VL, whose reasoning capabilities improve with an increase in parameters when the number of parameters is small, the reasoning capabilities of other models remain relatively stable once the number of parameters reaches a certain threshold. This suggests that increasing the number of parameters primarily enhances the knowledge capacity of models, with limited impact on improving specific reasoning abilities.

Table 7: Additional performance evaluation of various VLMs, including **BERTScore precision and recall**. “-” indicates that the model is unable to output a normal CoT reasoning, resulting in a negative BERTScore. **Boldface** indicates the best overall across all models. **Peach** and **Lemon** denote the best and the second-best among open-source models, respectively.

Model	QA		SU		OD		DM		EM		Overall	
	Precision	Recall										
Proprietary Large Vision-Language Models												
Claude-Sonnet-4.5	48.38	48.48	44.11	43.67	47.26	44.45	47.53	43.18	46.17	42.13	46.70	44.78
Gemini-2.5-pro [39]	27.56	43.82	24.15	38.12	26.34	38.42	26.82	39.50	27.16	37.55	26.28	39.83
GPT-4.1 [1]	53.71	50.54	51.13	45.77	52.58	44.15	54.12	44.35	50.57	40.96	52.61	45.87
GPT-5 [21]	36.46	24.74	37.55	22.07	35.52	17.73	37.53	19.15	39.53	19.17	37.06	20.98
Open-Source Large Vision-Language Models												
DeepSeek-VL2 [28]	9.01	-	3.31	-	3.66	-	-	-	0.74	-	2.36	-
DeepSeek-VL2-small [28]	-	6.28	-	1.34	-	-	-	0.17	-	-	-	-
DeepSeek-VL2-tiny [28]	26.03	-	16.07	-	19.46	-	19.32	-	10.37	-	19.33	-
InternVL2-2B [8]	36.16	16.53	32.56	19.14	36.03	14.29	35.00	13.86	31.98	10.01	34.60	15.55
InternVL2-4B [8]	44.50	34.48	42.28	27.64	39.00	23.04	43.19	25.75	39.83	24.12	42.11	27.69
InternVL2-8B [8]	47.42	30.74	43.92	32.52	44.59	28.85	45.17	27.46	43.65	28.52	45.15	29.92
InternVL2-26B [8]	47.58	30.60	49.80	33.32	47.06	25.25	49.13	26.92	47.20	25.41	48.30	28.94
InternVL3-2B [8]	42.87	32.52	33.28	19.27	33.50	19.50	37.73	19.70	38.04	23.84	37.08	23.16
InternVL3-8B [8]	39.34	30.93	30.28	24.96	36.27	25.87	33.64	23.26	32.93	24.81	34.70	26.28
InternVL3-14B [8]	41.98	35.01	31.70	23.23	39.15	30.02	39.27	28.37	37.25	28.65	37.84	29.11
InternVL3-38B [8]	47.16	34.25	43.23	30.88	44.66	28.92	43.65	27.30	43.36	27.87	44.60	30.31
Llama-4-Scout-17B-16E-Instruct [40]	43.10	44.26	35.64	38.33	38.83	41.87	41.77	40.61	39.10	38.26	39.72	40.98
LLaVA-NeXT-7B-Mistral [26]	41.00	19.35	39.95	16.96	37.17	13.96	39.65	17.28	40.47	17.39	39.64	17.05
LLaVA-NeXT-8B [26]	44.01	26.03	45.89	25.98	42.42	18.53	45.84	23.13	41.75	21.25	44.30	23.44
LLaVA-NeXT-13B [26]	15.48	5.85	28.00	12.30	28.61	7.20	26.04	8.16	26.05	9.68	24.41	8.57
LLaVA-NeXT-34B [26]	30.93	22.23	44.59	21.64	43.43	21.44	42.19	18.72	43.73	21.85	40.38	21.18
Qwen2.5-VL-3B-Instruct [3]	39.43	24.39	33.88	21.95	36.16	14.54	35.14	14.76	35.42	17.83	36.13	19.21
Qwen2.5-VL-7B-Instruct [3]	41.17	27.44	36.56	25.40	36.45	16.36	37.85	16.81	38.18	15.36	38.11	21.36
Qwen2.5-VL-32B-Instruct [3]	27.80	34.98	25.52	34.87	25.34	31.66	23.93	31.79	26.32	34.59	25.82	33.60
TinyLLaVA-1.5B [57]	31.97	-	19.61	-	26.61	-	22.00	-	23.80	-	25.01	-
TinyLLaVA-2B [57]	7.50	-	23.55	-	13.27	-	7.88	-	12.81	-	13.25	-
TinyLLaVA-3.1B [57]	26.08	-	24.41	-	21.86	-	22.36	-	27.86	-	24.24	-

5.2 Are VLMs capable of handling deep reasoning tasks?

As shown in Fig. 6, the performance of various models across different ROUGE and BERTScore metrics (precision, recall, and F1 score) demonstrates how reasoning steps impact model performance. The recall scores notably decrease as the number of reasoning steps increases, suggesting that longer reasoning chains lead to more gaps in the model’s coverage. This implies that while the model may accurately capture key information in the initial steps, it struggles to maintain comprehensive reasoning over longer chains. Conversely, precision remains relatively stable, and in some cases, even increases as the number of steps grows. This indicates that while the models are able to generate more specific and accurate responses in later reasoning steps, they may be sacrificing breadth for accuracy, leading to fewer but more focused answers. Overall, these changes result in a decrease in F1 score as the reasoning steps increase. This is because F1 score balances precision and recall, and the decline in recall outweighs the relatively stable performance of precision. This trend underscores a common challenge in reasoning tasks that models may be able to generate precise answers, but as the complexity of the reasoning process increases, they struggle to maintain comprehensive coverage, leading to a trade-off between precision and recall.

Table 8: Additional performance evaluation of VLMs using **accuracy** across different second-level tasks. Abbreviations adopted: OC for Organism Counting; RC for Regional Counting, MS for Morphological Statistics; BA for Boundary Analysis; AE for Area Evaluation; SR for Spatial Relationship; OI for Organism Identification; AD for Anomaly Detection; PM for Plant Management; PR for Pest Recognition; BI for BioMorph Identification; DD for Disease Diagnosis; AT for Agri-Tools; AM for Agri-Methods; MD for Management Decisions. **Boldface** indicates the best overall across all models. **Peach** and **Lemon** denote the best and the second-best among open-source models, respectively.

Model	OC	QA RC	MS	BA	SU AE	SR	OI	OD AD	PM	PR	DM BI	DD	AT	EM AM	MD
Proprietary Large Vision-Language Models															
Claude-Sonnet-4.5	48.80	3.88	47.27	37.56	48.59	52.24	70.75	57.43	76.04	67.67	79.63	62.10	81.54	83.47	61.07
Gemini-2.5-pro [39]	44.28	17.48	46.99	41.37	48.78	68.16	82.78	41.40	79.17	73.31	88.89	66.42	93.85	90.08	79.01
GPT-4.1 [1]	43.07	18.45	45.90	39.34	52.35	59.20	80.71	51.02	78.12	71.80	87.04	69.23	90.77	87.60	72.90
GPT-5 [21]	52.41	17.48	56.83	44.42	57.82	64.18	82.16	51.31	76.04	75.56	90.74	74.11	96.92	87.60	71.76
Open-Source Large Vision-Language Models															
DeepSeek-VL2 [28]	28.92	62.14	15.57	11.68	22.03	5.97	24.48	19.24	13.54	7.52	35.19	19.70	47.69	34.71	22.52
DeepSeek-VL2-small [28]	33.43	30.10	35.25	9.90	22.60	8.46	28.63	37.61	12.50	6.39	42.59	33.96	49.23	39.67	19.85
DeepSeek-VL2-tiny [28]	21.84	14.56	12.02	9.14	25.61	5.97	31.95	16.62	7.29	16.17	33.33	31.71	33.85	29.75	32.82
InternVL2-2B [8]	32.08	59.22	39.07	8.88	24.11	13.43	22.82	42.57	14.58	7.52	47.22	36.21	38.46	43.80	24.81
InternVL2-4B [8]	29.67	5.83	15.30	28.43	25.42	6.47	45.85	25.36	30.21	22.93	46.30	47.47	33.85	46.28	41.98
InternVL2-8B [8]	40.51	48.54	30.60	30.96	42.37	51.24	50.41	66.18	41.67	61.28	59.26	39.96	53.85	61.98	45.04
InternVL2-26B [8]	49.55	43.69	30.33	29.19	39.17	47.76	67.01	44.61	38.54	63.53	75.93	47.28	64.62	71.90	66.03
InternVL3-2B [8]	34.34	69.90	27.32	16.24	45.57	39.30	36.31	51.90	26.04	9.77	55.56	36.02	58.46	58.68	30.92
InternVL3-8B [8]	43.22	22.33	25.14	33.25	41.43	53.73	59.13	69.97	58.33	62.78	71.30	49.72	66.15	74.38	48.85
InternVL3-14B [8]	48.95	60.19	45.08	38.07	48.21	48.26	58.92	63.27	76.04	68.42	68.52	60.60	70.77	80.17	64.50
InternVL3-38B [8]	55.42	32.04	34.97	39.59	47.65	52.74	75.31	66.47	81.25	66.92	73.15	64.92	70.77	78.51	68.32
Llama-4-Scout-17B-16E-Instruct [40]	50.15	9.71	32.24	34.77	42.75	42.29	68.67	51.31	64.58	65.79	68.52	64.17	72.31	80.99	55.34
LLaVA-NeXT-7B-Mistral [26]	17.32	73.79	33.06	7.36	20.90	12.94	31.33	9.62	21.88	31.20	37.96	19.70	44.62	50.41	32.82
LLaVA-NeXT-8B [26]	31.93	71.84	41.26	31.98	16.38	25.87	43.15	23.62	41.67	59.40	31.48	34.33	40.00	47.11	33.97
LLaVA-NeXT-13B [26]	8.89	25.24	8.47	8.12	18.08	11.44	14.32	7.29	10.42	7.14	14.81	17.07	24.62	21.49	13.36
LLaVA-NeXT-34B [26]	49.10	67.96	45.08	36.80	15.63	52.74	41.91	66.18	39.58	60.53	33.33	29.46	50.77	54.55	41.98
Qwen2.5-VL-3B-Instruct [3]	43.52	14.56	19.95	33.76	36.35	52.24	56.64	65.01	72.92	57.52	63.89	55.91	58.46	57.85	44.27
Qwen2.5-VL-7B-Instruct [3]	48.34	4.85	30.87	28.68	36.16	49.25	64.32	62.39	56.25	67.29	76.85	49.34	69.23	63.64	43.51
Qwen2.5-VL-32B-Instruct [3]	38.40	18.45	32.24	8.63	20.90	11.44	20.12	8.75	15.62	7.14	28.70	19.14	27.69	37.19	15.27
TinyLLaVA-1.5B [57]	23.64	25.24	10.38	13.45	18.64	5.97	27.18	7.29	8.33	7.89	36.11	33.02	32.31	29.75	14.50
TinyLLaVA-2B [57]	43.07	0.00	28.69	28.17	24.86	6.97	64.11	20.70	37.50	53.01	40.74	44.47	41.54	43.80	39.69
TinyLLaVA-3.1B [57]	38.55	13.59	30.05	23.86	19.40	8.46	58.30	12.83	62.50	42.86	45.37	38.46	47.69	61.16	39.31

6 Dimension Details and Case Study

In this section, we present a series of task-specific question examples from AgroCoT, paired with responses generated by GPT-4.1 and InternVL3-38B (refer to Fig. 7 through Fig. 21 for details). For clarity, text colors in the figures are assigned specific meanings: **red** denotes question extraction, **brown** represents key analysis, and **green** indicates answer summary.

Although GPT-5 gets highest accuracy score, GPT-4.1 stands out as the top-performing proprietary model in our AgroCoT evaluations. On the open-source side, InternVL3-38B emerges as the strongest model in our assessment, achieving the highest overall accuracy among publicly accessible VLMs. By comparing these two systems, we aim to illustrate both the upper performance threshold of modern VLMs and the advancement of open-source alternatives. These case examples span the full range of AgroCoT’s task dimensions: each case includes a visual input (three views: satellite, aerial, or ground-level imagery), a task-aligned query, and the corresponding reasoning and answers generated by the models.

Table 9: Additional performance evaluation of VLMs using **ROUGE-L F1** across different second-level tasks. Abbreviations adopted: OC for Organism Counting; RC for Regional Counting; MS for Morphological Statistics; BA for Boundary Analysis; AE for Area Evaluation; SR for Spatial Relationship; OI for Organism Identification; AD for Anomaly Detection; PM for Plant Management; PR for Pest Recognition; BI for BioMorph Identification; DD for Disease Diagnosis; AT for Agri-Tools; AM for Agri-Methods; MD for Management Decisions. **Boldface** indicates the best overall across all models. **Peach** and **Lemon** denote the best and the second-best among open-source models, respectively.

Model	QA			SU			OD			DM			EM		
	OC	RC	MS	BA	AE	SR	OI	AD	PM	PR	BI	DD	AT	AM	MD
Proprietary Large Vision-Language Models															
Claude-Sonnet-4.5	47.71	47.47	45.86	41.91	41.08	42.63	48.08	42.67	45.24	47.73	48.09	44.63	42.73	44.11	45.56
Gemini-2.5-pro [39]	37.15	32.74	36.04	33.22	31.90	34.70	36.35	32.90	36.94	38.33	37.91	35.76	36.11	36.72	36.00
GPT-4.1 [1]	51.31	50.98	50.44	45.25	46.39	44.13	51.10	43.53	49.76	54.09	48.64	47.89	44.50	44.17	48.25
GPT-5 [21]	29.58	31.14	31.91	26.77	28.12	27.40	29.26	26.88	27.04	31.69	29.55	28.02	27.75	27.36	29.09
Open-Source Large Vision-Language Models															
DeepSeek-VL2 [28]	19.13	21.94	9.23	16.01	4.63	1.76	10.68	12.45	18.81	21.91	3.75	7.18	2.79	3.93	8.61
DeepSeek-VL2-small [28]	19.31	16.12	12.86	12.56	5.28	5.29	15.56	9.67	8.27	20.10	7.67	13.70	6.71	8.32	14.80
DeepSeek-VL2-tiny [28]	19.19	24.69	10.24	8.23	7.20	2.97	13.43	13.71	13.07	19.24	2.09	7.65	1.59	1.32	8.21
InternVL2-2B [8]	27.64	28.34	31.71	29.38	28.01	30.15	27.34	30.44	34.53	29.00	31.15	28.60	30.91	30.30	26.05
InternVL2-4B [8]	40.03	36.72	41.70	33.55	36.80	32.74	36.42	32.09	30.80	42.99	34.07	34.12	32.66	34.24	35.24
InternVL2-8B [8]	38.04	37.81	38.27	37.85	38.99	37.65	37.50	37.73	35.78	42.41	37.30	36.70	35.18	35.22	40.51
InternVL2-26B [8]	37.97	28.10	42.82	39.05	40.15	39.35	40.17	38.85	32.28	41.50	37.57	37.71	33.69	34.27	39.81
InternVL3-2B [8]	40.04	36.10	40.21	30.46	37.57	33.21	36.23	32.40	31.47	37.20	35.28	33.37	36.25	37.43	37.06
InternVL3-8B [8]	42.40	39.44	43.97	39.56	39.72	37.44	37.53	40.64	36.31	43.36	39.76	37.45	36.50	38.67	42.74
InternVL3-14B [8]	45.86	50.81	45.64	39.58	39.62	34.90	40.43	41.82	43.31	44.36	42.43	39.00	38.03	37.44	43.03
InternVL3-38B [8]	44.37	43.40	44.43	39.43	39.13	34.48	38.91	39.18	41.04	42.56	39.34	37.44	35.87	36.39	40.80
Llama-4-Scout-17B-16E-Instruct [40]	46.25	40.95	43.60	38.60	38.10	38.98	42.88	37.99	42.33	43.15	42.59	43.68	39.49	41.30	41.77
LLaVA-NeXT-7B-Mistral [26]	28.67	24.02	41.45	30.96	32.35	33.24	30.47	29.70	34.51	36.74	28.36	31.86	29.73	32.15	30.81
LLaVA-NeXT-8B [26]	29.49	34.42	43.83	36.78	36.72	39.16	33.43	35.15	30.22	36.47	32.53	36.32	34.33	34.53	33.38
LLaVA-NeXT-13B [26]	22.61	26.36	24.23	27.02	25.90	27.86	28.62	25.69	16.25	29.18	23.36	26.56	24.63	26.61	25.96
LLaVA-NeXT-34B [26]	30.24	32.93	35.38	35.34	36.97	22.05	29.78	36.09	38.84	34.86	29.40	33.13	30.35	30.86	36.30
Qwen2.5-VL-3B-Instruct [3]	32.03	35.12	32.45	31.06	31.01	29.83	29.09	28.99	30.96	31.19	28.64	29.11	30.16	30.71	32.72
Qwen2.5-VL-7B-Instruct [3]	36.67	30.78	37.11	31.10	35.32	34.27	32.71	29.51	34.16	35.08	32.74	31.85	31.80	33.32	30.32
Qwen2.5-VL-32B-Instruct [3]	36.99	41.60	34.89	33.12	33.34	33.89	33.21	33.38	38.47	36.72	35.93	34.05	36.10	36.28	36.00
TinyLLaVA-1.5B [57]	18.62	23.43	16.26	10.77	7.15	1.96	9.12	14.29	11.84	13.89	5.32	6.62	7.17	8.07	12.08
TinyLLaVA-2B [57]	1.99	1.17	6.95	7.80	5.25	2.51	1.88	8.96	5.65	0.59	1.77	5.23	2.12	1.76	6.94
TinyLLaVA-3.1B [57]	14.45	13.24	19.79	10.76	13.55	13.01	11.95	12.27	10.18	6.74	14.42	11.41	16.60	14.66	12.21

Our analysis of these examples reveals that GPT-4.1 exhibits more structured reasoning processes—though its outputs lean toward greater verbosity—paired with broader knowledge coverage, which contributes to higher answer accuracy (especially in tasks requiring complex reasoning or spatial interpretation). In contrast, InternVL3-38B delivers more concise, efficient reasoning and performs competently in visual recognition and straightforward classification tasks. However, it occasionally shows gaps in knowledge reserve and struggles with nuanced spatial relationships or logical inference, resulting in slightly lower overall answer accuracy. These distinctions reflect the varying levels of generalization capability and domain adaptability across contemporary VLMs.

To ensure that models effectively utilize visual information during reasoning, the AgroCoT dataset’s reasoning chains explicitly integrate spatial localization mechanisms. As shown in Fig. 10, each reasoning chain includes references to specific image regions in key steps, guiding the model to accurately locate relevant visual evidence when answering questions. This design not only enhances the interpretability of the reasoning process but also encourages the model to establish a tighter interaction between the visual and textual modalities, preventing vague reasoning disconnected from the image content. The example in Fig. 10

Table 10: Additional performance evaluation of VLMs using **BERTScore F1** across different second-level tasks. “-” indicates that the model is unable to output a normal CoT reasoning, resulting in a negative BERTScore. Abbreviations adopted: OC for Organism Counting; RC for Regional Counting, MS for Morphological Statistics; BA for Boundary Analysis; AE for Area Evaluation; SR for Spatial Relationship; OI for Organism Identification; AD for Anomaly Detection; PM for Plant Management; PR for Pest Recognition; BI for BioMorph Identification; DD for Disease Diagnosis; AT for Agri-Tools; AM for Agri-Methods; MD for Management Decisions. **Boldface** indicates the best overall across all models. **Peach** and **Lemon** denote the best and the second-best among open-source models, respectively.

Model	QA			SU			OD			DM			EM		
	OC	RC	MS	BA	AE	SR	OI	AD	PM	PR	BI	DD	AT	AM	MD
Proprietary Large Vision-Language Models															
Claude-Sonnet-4.5	48.53	53.44	46.89	42.26	45.03	42.67	48.70	43.55	47.44	48.65	47.17	43.33	39.70	40.71	46.80
Gemini-2.5-pro [39]	36.21	36.93	33.55	29.49	30.51	36.75	33.79	29.36	34.29	36.25	33.23	31.38	29.59	29.97	34.00
GPT-4.1 [1]	52.20	54.85	51.23	45.81	50.03	46.54	51.91	45.15	51.86	54.84	47.76	46.54	42.29	40.33	48.86
GPT-5 [21]	29.08	33.37	32.07	24.88	31.45	31.25	28.52	26.47	21.51	32.83	26.55	25.76	25.31	25.93	30.96
Open-Source Large Vision-Language Models															
DeepSeek-VL2 [28]	-	3.05	-	-	-	-	-	-	-	2.23	-	-	-	-	-
DeepSeek-VL2-small [28]	-	2.91	-	-	-	-	-	-	-	-	-	-	-	-	-
DeepSeek-VL2-tiny [28]	11.29	27.19	-	-	-	-	-	-	-	12.73	-	-	-	-	-
InternVL2-2B [8]	24.50	26.49	27.62	23.86	25.65	30.47	21.75	26.66	24.81	26.50	24.38	22.29	24.80	22.57	17.75
InternVL2-4B [8]	38.73	40.87	40.11	29.44	37.56	35.86	34.57	28.54	24.88	42.76	30.43	30.47	28.61	29.75	33.26
InternVL2-8B [8]	38.18	39.78	39.45	34.97	40.04	37.12	37.39	38.15	30.47	42.79	32.73	33.18	31.36	30.41	39.32
InternVL2-26B [8]	37.97	28.52	43.09	36.84	41.58	42.16	39.15	37.58	25.79	43.09	33.56	35.39	31.03	30.16	39.36
InternVL3-2B [8]	37.95	38.41	36.57	22.90	25.67	34.92	26.52	25.31	25.17	33.39	27.08	25.93	27.69	26.11	33.41
InternVL3-8B [8]	36.49	40.84	30.87	31.36	23.16	30.40	29.57	35.10	24.87	37.18	25.82	24.46	20.03	19.85	35.05
InternVL3-14B [8]	38.33	52.39	34.74	27.82	26.60	31.58	36.02	31.75	36.06	40.59	32.20	30.57	26.85	28.20	36.43
InternVL3-38B [8]	41.43	43.00	38.18	35.71	38.21	33.90	36.88	37.39	36.06	40.48	34.61	32.64	32.38	32.04	37.50
Llama-4-Scout-17B-16E-Instruct [40]	44.46	42.27	42.52	34.93	38.72	40.04	42.36	36.46	40.26	41.04	39.23	41.64	35.98	37.76	39.69
LLaVA-NeXT-7B-Mistral [26]	27.26	15.28	37.68	25.83	26.86	31.15	26.92	22.51	28.92	33.22	20.88	26.58	24.60	26.89	29.77
LLaVA-NeXT-8B [26]	30.05	36.39	42.22	34.00	33.72	40.00	30.83	31.49	22.10	35.40	28.38	34.12	31.50	29.41	31.58
LLaVA-NeXT-13B [26]	9.33	12.82	12.28	20.57	20.24	13.78	21.92	16.35	4.48	14.28	12.42	18.63	19.01	20.41	15.49
LLaVA-NeXT-34B [26]	23.68	32.11	29.82	32.52	37.70	14.76	27.53	37.69	36.78	35.80	25.36	27.64	27.99	26.49	35.91
Qwen2.5-VL-3B-Instruct [3]	31.42	38.15	30.27	27.32	29.07	24.26	23.70	25.20	24.37	28.95	21.09	22.85	23.58	23.40	28.03
Qwen2.5-VL-7B-Instruct [3]	34.43	38.22	32.30	25.35	33.20	35.48	26.48	23.86	27.62	31.75	26.18	24.40	25.43	25.73	26.19
Qwen2.5-VL-32B-Instruct [3]	30.30	39.91	30.17	25.46	31.06	36.23	28.53	28.21	31.32	27.25	30.85	27.16	29.90	30.49	30.45
TinyLLaVA-1.5B [57]	11.87	24.27	0.40	-	-	-	-	2.70	0.71	11.36	-	-	-	-	-
TinyLLaVA-2B [57]	-	-	-	-	-	-	-	-	-	-	-	-	-	-	-
TinyLLaVA-3.1B [57]	3.19	5.22	7.53	-	1.98	1.22	-	-	-	-	1.12	0.17	5.80	4.20	0.70

further demonstrates that, through this structured spatial guidance, the model can more accurately focus on the correct visual areas, thereby improving the reliability of the answer.

7 Limitations and Future Work

Although AgroCoT provides a multi-dimensional perspective for evaluating the reasoning capabilities of vision-language models in the agricultural domain, this study has certain limitations. Currently, we have not systematically explored the extent to which the introduction of Chain-of-Thought (CoT) reasoning directly improves the accuracy of model answers. Specifically, the causal contribution of CoT reasoning to the final task performance has yet to be quantified. Additionally, in the highly specialized field of agriculture, further research is needed to design more effective CoT guidance strategies that can better help vision-language models integrate domain knowledge and visual evidence, while addressing the reasoning challenges present in complex agricultural scenarios.

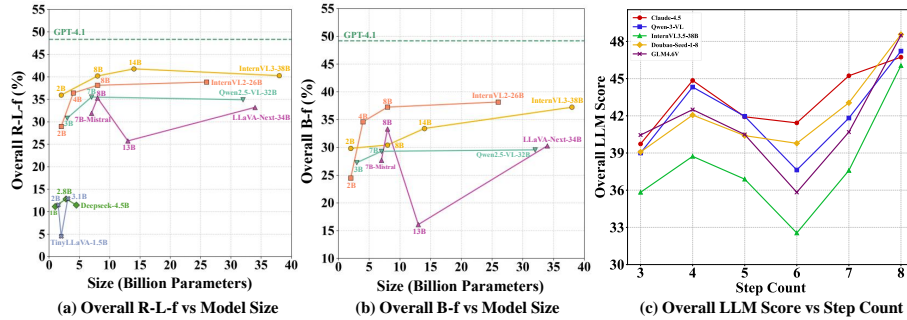


Fig. 5: ROUGE-L F1 (a) and BERTScore F1 (b) vary with model parameter size, and LLM scores (c) vary with reasoning step counts.

While AgroCoT has been carefully curated and manually refined to address agricultural VQA tasks, the current dataset scale remains insufficient given the rapid evolution of modern VLMs. As model capacities continue to grow, larger and more diverse training data become essential to fully exploit their reasoning potential. Therefore, AgroCoT will be progressively expanded by incorporating additional high-quality samples covering broader crop varieties, cultivation practices, environmental conditions, and region-specific scenarios.

8 Ethical Considerations

The AgroCoT dataset is built upon publicly available open-source datasets, with the exception of a small amount of privately created data. All other data is sourced from published academic resources and is used in strict compliance with the corresponding dataset’s copyright statements and licensing terms. We commit to releasing the AgroCoT dataset as an open-source project, aimed at advancing research in the field of agricultural artificial intelligence and promoting reproducible evaluation and model iteration.

The 20 annotators complete training covering agricultural knowledge, annotation protocols, and ethical norms. Participation is voluntary, participants’ right to information is guaranteed, and rest breaks are provided during annotation. All annotators receive specialized ethics training and take scheduled rest breaks to prevent contamination of the dataset during the refinement of CoTs. After annotation is completed, a dedicated ethics review of CoT content is conducted to identify and address any potential issues.

References

1. Achiam, J., Adler, S., Agarwal, S., Ahmad, L., Akkaya, I., Aleman, F.L., Almeida, D., Altenschmidt, J., Altman, S., Anadkat, S., et al.: Gpt-4 technical report. arXiv preprint arXiv:2303.08774 (2023)

2. Awais, M., Alharthi, A.H.S.A., Kumar, A., Cholakkal, H., Anwer, R.M.: Agrogpt: Efficient agricultural vision-language model with expert tuning. In: 2025 IEEE/CVF Winter Conference on Applications of Computer Vision (WACV). pp. 5687–5696. IEEE (2025)
3. Bai, J., Bai, S., Yang, S., Wang, S., Tan, S., Wang, P., Lin, J., Zhou, C., Zhou, J.: Qwen-vl: A frontier large vision-language model with versatile abilities. arXiv preprint arXiv:2308.12966 **1**(2), 3 (2023)
4. Bai, S., Chen, K., Liu, X., Wang, J., Ge, W., Song, S., Dang, K., Wang, P., Wang, S., Tang, J., et al.: Qwen2. 5-vl technical report. arXiv preprint arXiv:2502.13923 (2025)
5. Bie, Y., Xu, G., Wang, Y.: Adapting vision-language models for precision agriculture: A study on crop segmentation based on uav remote sensing data. In: 2025 13th International Conference on Agro-Geoinformatics (Agro-Geoinformatics). pp. 1–6 (2025)
6. Cao, Y., Chen, L., Yuan, Y., Sun, G.: Cucumber disease recognition with small samples using image-text-label-based multi-modal language model. *Computers and electronics in agriculture* **211**, 107993 (2023)
7. Chen, Q., Qin, L., Zhang, J., Chen, Z., Xu, X., Che, W.: M3cot: A novel benchmark for multi-domain multi-step multi-modal chain-of-thought. In: Proceedings of the 62nd Annual Meeting of the Association for Computational Linguistics (Volume 1: Long Papers). pp. 8199–8221 (2024)
8. Chen, Z., Wang, W., Cao, Y., Liu, Y., Gao, Z., Cui, E., Zhu, J., Ye, S., Tian, H., Liu, Z., et al.: Expanding performance boundaries of open-source multimodal models with model, data, and test-time scaling. arXiv preprint arXiv:2412.05271 (2024)
9. Cheng, Z., Chen, Q., Zhang, J., et al.: Comt: A novel benchmark for chain of multi-modal thought on large vision-language models. In: AAAI. pp. 23678–23686 (2025)
10. Comanici, G., Bieber, E., Schaekermann, M., Pasupat, I., Sachdeva, N., Dhillon, I., Blistein, M., Ram, O., Zhang, D., Rosen, E., et al.: Gemini 2.5: Pushing the frontier with advanced reasoning, multimodality, long context, and next generation agentic capabilities. arXiv preprint arXiv:2507.06261 (2025)
11. Dongre, V., Gui, C., Garg, S., Nayyeri, H., Tur, G., Hakkani-Tür, D., Adve, V.S.: Mirage: A benchmark for multimodal information-seeking and reasoning in agricultural expert-guided conversations. arXiv preprint arXiv:2506.20100 (2025)
12. Gao, J., Li, Y., Cao, Z., Li, W.: Interleaved-modal chain-of-thought. In: Proceedings of the Computer Vision and Pattern Recognition Conference. pp. 19520–19529 (2025)
13. Gao, M., Liu, X., Yue, Z., Wu, Y., Chen, S., Li, J., Tang, S., Wu, F., Chua, T.S., Zhuang, Y.: Benchmarking multimodal cot reward model stepwise by visual program. arXiv preprint arXiv:2504.06606 (2025)
14. Gauba, A., Pi, I., Man, Y., Pang, Z., Adve, V.S., Wang, Y.X.: Agmmu: A comprehensive agricultural multimodal understanding benchmark. In: The Thirty-ninth Annual Conference on Neural Information Processing Systems Datasets and Benchmarks Track (2025)
15. Guo, M.H., Chu, X., Yang, Q., Mo, Z.H., Shen, Y., Li, P.L., Lin, X., Zhang, J., Chen, X.S., Zhang, Y., et al.: Rbench-v: A primary assessment for visual reasoning models with multi-modal outputs. arXiv preprint arXiv:2505.16770 (2025)
16. Hao, Y., Gu, J., Wang, H.W., Li, L., Yang, Z., Wang, L., Cheng, Y.: Can mllms reason in multimodality? emma: An enhanced multimodal reasoning benchmark. arXiv preprint arXiv:2501.05444 (2025)

17. Hong, W., Yu, W., Gu, X., Wang, G., Gan, G., Tang, H., Cheng, J., Qi, J., Ji, J., Pan, L., et al.: Glm-4.5 v and glm-4.1 v-thinking: Towards versatile multimodal reasoning with scalable reinforcement learning. arXiv preprint arXiv:2507.01006 (2025)
18. Hurst, A., Lerer, A., Goucher, A.P., Perelman, A., Ramesh, A., Clark, A., Ostrow, A., Welihinda, A., Hayes, A., Radford, A., et al.: Gpt-4o system card. arXiv preprint arXiv:2410.21276 (2024)
19. Jiang, D., et al.: Mme-cot: Benchmarking chain-of-thought in large multimodal models for reasoning quality, robustness, and efficiency. arXiv preprint arXiv:2502.09621 (2025)
20. Kojima, T., Gu, S.S., Reid, M., Matsuo, Y., Iwasawa, Y.: Large language models are zero-shot reasoners. *Advances in neural information processing systems* **35**, 22199–22213 (2022)
21. Leon, M.: Gpt-5 and open-weight large language models: Advances in reasoning, transparency, and control. *Information Systems* p. 102620 (2025)
22. Li, Q., Zhang, Y., Mai, Z., Chen, Y., Lou, S., Huang, H., Zhang, J., Zhang, Z., Wen, Y., Li, W., et al.: Can large multimodal models understand agricultural scenes? benchmarking with agromind. arXiv preprint arXiv:2505.12207 (2025)
23. Li, Z., Chang, Y., Wu, Y.: Think-bench: Evaluating thinking efficiency and chain-of-thought quality of large reasoning models. arXiv preprint arXiv:2505.22113 (2025)
24. Li, Z., Wu, X., Du, H., Nghiem, H., Shi, G.: A survey of state of the art large vision language models: Alignment, benchmark, evaluations and challenges. arXiv preprint arXiv:2501.02189 1 (2025)
25. Liu, A., Feng, B., Xue, B., Wang, B., Wu, B., Lu, C., Zhao, C., Deng, C., Zhang, C., Ruan, C., et al.: Deepseek-v3 technical report. arXiv preprint arXiv:2412.19437 (2024)
26. Liu, H., Li, C., Li, Y., Lee, Y.J.: Improved baselines with visual instruction tuning. In: *Proceedings of the IEEE/CVF conference on computer vision and pattern recognition*. pp. 26296–26306 (2024)
27. Liu, X., Liu, Z., Hu, H., Chen, Z., Wang, K., Wang, K., Lian, S.: A multimodal benchmark dataset and model for crop disease diagnosis. In: *European Conference on Computer Vision*. pp. 157–170. Springer (2024)
28. Lu, H., Liu, W., Zhang, B., Wang, B., Dong, K., Liu, B., Sun, J., Ren, T., Li, Z., Yang, H., et al.: Deepseek-vl: towards real-world vision-language understanding. arXiv preprint arXiv:2403.05525 (2024)
29. Lu, P., Bansal, H., Xia, T., Liu, J., Li, C., Hajishirzi, H., Cheng, H., Chang, K.W., Galley, M., Gao, J.: Mathvista: Evaluating mathematical reasoning of foundation models in visual contexts. arXiv preprint arXiv:2310.02255 (2023)
30. Lu, P., Mishra, S., Xia, T., Qiu, L., Chang, K.W., Zhu, S.C., Tafjord, O., Clark, P., Kalyan, A.: Learn to explain: Multimodal reasoning via thought chains for science question answering. *Advances in Neural Information Processing Systems* **35**, 2507–2521 (2022)
31. Mitra, C., Huang, B., Darrell, T., Herzig, R.: Compositional chain-of-thought prompting for large multimodal models. In: *Proceedings of the IEEE/CVF Conference on Computer Vision and Pattern Recognition*. pp. 14420–14431 (2024)
32. Qian, Y., Wan, C., Jia, C., Yang, Y., Zhao, Q., Gan, Z.: Prism-bench: A benchmark of puzzle-based visual tasks with cot error detection. arXiv preprint arXiv:2510.23594 (2025)

33. Radford, A., Kim, J.W., Hallacy, C., Ramesh, A., Goh, G., Agarwal, S., Sastry, G., Askell, A., Mishkin, P., Clark, J., Krueger, G., Sutskever, I.: Learning transferable visual models from natural language supervision. In: Meila, M., Zhang, T. (eds.) *Proceedings of the 38th International Conference on Machine Learning*. *Proceedings of Machine Learning Research*, vol. 139, pp. 8748–8763. PMLR (18–24 Jul 2021)
34. Schwenk, D., Khandelwal, A., Clark, C., Marino, K., Mottaghi, R.: A-okvqa: A benchmark for visual question answering using world knowledge. In: *European conference on computer vision*. pp. 146–162. Springer (2022)
35. Seed, B.: Seed1. 8 model card: Towards generalized real-world agency. Tech. rep., 2025a. Technical Report (2025)
36. Shaikh, T.A., Rasool, T., Veningston, K., Yaseen, S.M.: The role of large language models in agriculture: harvesting the future with LLM intelligence. *Progress in Artificial Intelligence* **14**(2), 117–164 (Jun 2025)
37. Shinoda, R., Inoue, N., Kataoka, H., Onishi, M., Ushiku, Y.: Agrobench: Vision-language model benchmark in agriculture. In: *Proceedings of the IEEE/CVF International Conference on Computer Vision*. pp. 7634–7644 (2025)
38. Singh, M., Cambronero, J., Gulwani, S., Le, V., Verbruggen, G.: Assessing gpt4-v on structured reasoning tasks. *arXiv preprint arXiv:2312.11524* (2023)
39. Team, G., Anil, R., Borgeaud, S., Alayrac, J.B., Yu, J., Soricut, R., Schalkwyk, J., Dai, A.M., Hauth, A., Millican, K., et al.: Gemini: a family of highly capable multimodal models. *arXiv preprint arXiv:2312.11805* (2023)
40. Touvron, H., Lavril, T., Izacard, G., Martinet, X., Lachaux, M.A., Lacroix, T., Rozière, B., Goyal, N., Hambro, E., Azhar, F., et al.: Llama: Open and efficient foundation language models. *arXiv preprint arXiv:2302.13971* (2023)
41. Wang, L., Jin, T., Yang, J., Leonardis, A., Wang, F., Zheng, F.: Agri-llava: Knowledge-infused large multimodal assistant on agricultural pests and diseases. *arXiv preprint arXiv:2412.02158* (2024)
42. Wang, X., Wei, J., Schuurmans, D., Le, Q., Chi, E., Narang, S., Chowdhery, A., Zhou, D.: Self-consistency improves chain of thought reasoning in language models. *arXiv preprint arXiv:2203.11171* (2022)
43. Wang, Y., Wu, S., Zhang, Y., Yan, S., Liu, Z., Luo, J., Fei, H.: Multimodal chain-of-thought reasoning: A comprehensive survey. *arXiv preprint arXiv:2503.12605* (2025)
44. Wang, Z., Zeng, X., Liu, W., Wang, Y., Li, L., Wang, Y., Shang, L., Jiang, X., Liu, Q., Wong, K.F.: Chain-of-probe: Examining the necessity and accuracy of cot step-by-step. In: *Findings of the Association for Computational Linguistics: NAACL 2025*. pp. 2586–2606 (2025)
45. Wei, J., Wang, X., Schuurmans, D., Bosma, M., Xia, F., Chi, E., Le, Q.V., Zhou, D., et al.: Chain-of-thought prompting elicits reasoning in large language models. *Advances in neural information processing systems* **35**, 24824–24837 (2022)
46. Wu, H., Mu, W., Zhong, D., Du, Z., Li, H., Tao, C.: Farmseg_vlm: A farmland remote sensing image segmentation method considering vision-language alignment. *ISPRS Journal of Photogrammetry and Remote Sensing* **225**, 423–439 (2025)
47. Yang, B., Chen, Y., Feng, L., Zhang, Y., Xu, X., Zhang, J., Aierken, N., Huang, R., Lin, H., Ying, Y., et al.: Agrigpt-vl: Agricultural vision-language understanding suite. *arXiv preprint arXiv:2510.04002* (2025)
48. Yao, S., Yu, D., Zhao, J., Shafran, I., Griffiths, T., Cao, Y., Narasimhan, K.: Tree of thoughts: Deliberate problem solving with large language models. *Advances in neural information processing systems* **36**, 11809–11822 (2023)

49. Yue, X., Ni, Y., Zhang, K., Zheng, T., Liu, R., Zhang, G., Stevens, S., Jiang, D., Ren, W., Sun, Y., et al.: Mmmu: A massive multi-discipline multimodal understanding and reasoning benchmark for expert agi. In: Proceedings of the IEEE/CVF Conference on Computer Vision and Pattern Recognition. pp. 9556–9567 (2024)
50. Zhang, H., Sun, J., Chen, R., Liu, W., Yuan, Z., Zheng, X., Wang, Z., Yang, Z., Yan, H., Zhong, H., et al.: Empowering and assessing the utility of large language models in crop science. *Advances in Neural Information Processing Systems* **37**, 52670–52722 (2024)
51. Zhang, K., Ma, L., Cui, B., Li, X., Zhang, B., Xie, N.: Visual large language model for wheat disease diagnosis in the wild. *Computers and Electronics in Agriculture* **227**, 109587 (2024)
52. Zhang, S., Hao, X., Tang, Y., Zhang, L., Wang, P., Wang, Z., Ma, H., Zhang, S.: Video-cot: A comprehensive dataset for spatiotemporal understanding of videos based on chain-of-thought. In: Proceedings of the 33rd ACM International Conference on Multimedia. pp. 12745–12752 (2025)
53. Zhang, Y., Chen, L., Yuan, Y.: Multimodal fine-grained transformer model for pest recognition. *Electronics* **12**(12), 2620 (2023)
54. Zhang, Y., Chen, L., Yuan, Y.: Few-shot agricultural pest recognition based on multimodal masked autoencoder. *Crop Protection* **187**, 106993 (2025)
55. Zhang, Y., Wang, X., Wu, L., Wang, J.: Enhancing chain of thought prompting in large language models via reasoning patterns. In: Proceedings of the AAAI Conference on Artificial Intelligence. pp. 25985–25993 (2025)
56. Zhao, X., Chen, B., Ji, M., Wang, X., Yan, Y., Zhang, J., Liu, S., Ye, M., Lv, C.: Implementation of large language models and agricultural knowledge graphs for efficient plant disease detection. *Agriculture* **14**(8), 1359 (2024)
57. Zhou, B., Hu, Y., Weng, X., Jia, J., Luo, J., Liu, X., Wu, J., Huang, L.: Tinyllava: A framework of small-scale large multimodal models. *arXiv preprint arXiv:2402.14289* (2024)
58. Zhou, Y., Yan, H., Ding, K., Cai, T., Zhang, Y.: Few-shot image classification of crop diseases based on vision–language models. *Sensors* **24**(18), 6109 (2024)

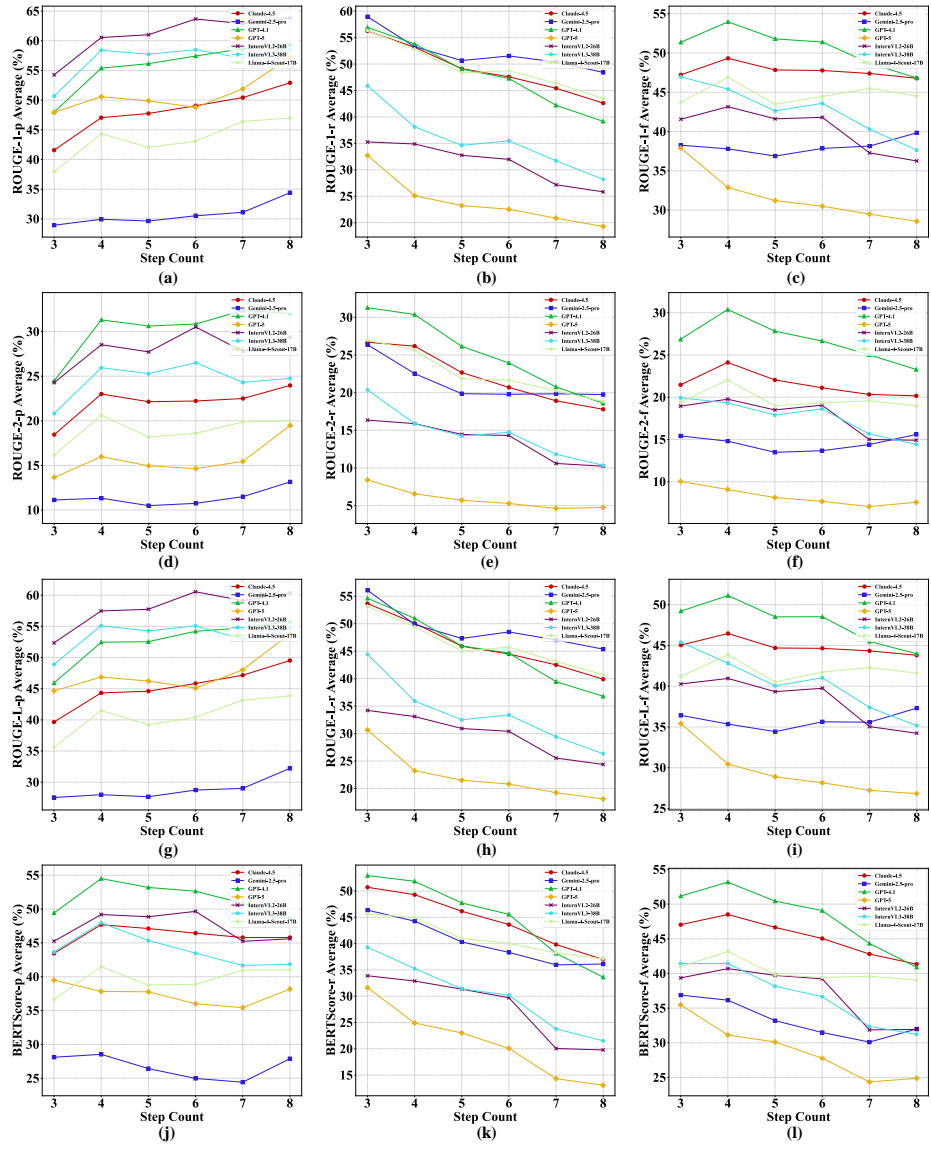


Fig. 6: Overall performance of several VLMs using ROUGE-1, ROUGE-2, ROUGE-L and BERTScore across different step counts.

Plant Management

Question: What type of damage is observed on the plant in the image?
Options: A: late season freeze-hail-freeze damage B: insect infestation damage
 C: bacterial leaf scorch D: early summer drought stress

Answer: A



Reasoning:

1. The question asks to identify the type of damage observed on the plant in the image, providing four options: late season freeze-hail-freeze damage, insect infestation damage, bacterial leaf scorch, and early summer drought stress.
2. Observing the image, the tree appears to have sparse foliage, with branches that are mostly bare and no visible signs of leaf scorch, insect activity, or drought-related wilting.
3. Late season freeze-hail-freeze damage is consistent with the observed symptoms, as freezing temperatures can cause buds and leaves to fail to develop properly, leaving the tree looking bare and stressed.
4. The other options (insect infestation, bacterial leaf scorch, and drought stress) typically show distinct signs such as holes in leaves, browning or scorching of leaf edges, or drooping foliage, none of which are visible in the image.
5. Based on the analysis, the most appropriate option is late season freeze-hail-freeze damage.

GPT-4.1: ✓ [bert_f1: 0.45] [rougeL_f: 0.49]

1. The question asks about the type of damage observed on the plant in the image, and provides four options related to different types of plant stress or damage. 2. Observing the image, the tree in the center appears to have no leaves, while the surrounding vegetation is green and healthy, indicating that the issue is specific to this tree and not a general environmental problem like drought. 3. There are no visible signs of insect infestation (such as holes, chewed leaves, or webs), nor are there symptoms of bacterial leaf scorch (which typically presents as browning leaf edges, not total leaf loss). 4. The tree's complete lack of leaves, while other plants are unaffected, suggests a sudden and severe event, such as a late season freeze or hail followed by another freeze, which can kill buds and young leaves, leading to a bare tree. 5. Therefore, the most appropriate answer is A: late season freeze-hail-freeze damage. **Answer: A**

InternVL3-38B: ✓ [bert_f1: 0.34] [rougeL_f: 0.41]

1. The plant in the image appears to have no leaves, which suggests it has experienced some form of damage or stress. 2. The branches are bare, indicating that the damage occurred after the leaves had already grown, which is more consistent with a late-season event. 3. The absence of visible insect damage or signs of bacterial infection (such as leaf spots or discoloration) makes options B and C less likely. 4. Early summer drought stress (option D) typically results in wilting or browning of leaves rather than complete defoliation. 5. A late-season freeze, hail, or freeze damage (option A) can cause sudden defoliation and matches the observed condition of the plant. **Answer: A**

Fig. 7: A case of the Plant Management task with responses from GPT-4.1 and InternVL3-38B.

Organism Identification

Question: What are the distinctive features of the plant shown in the image?
Options: A: pine tree with needle-like leaves and brown cones B: cactus with thick, spiny stems and no leaves
 C: ostrich fern with arching habit and tough, wiry black rhizomes D: bamboo with straight stalks and green leaves

Answer: C



Reasoning:

1. The question asks to identify the distinctive features of the plant shown in the image and match it with the most appropriate option.
2. The image depicts a plant with arching fronds, characteristic of ferns, and some parts of the plant show wiry, dark structures resembling rhizomes.
3. Option A describes a pine tree with needle-like leaves and brown cones, which does not match the plant in the image as the plant lacks needle-like leaves or cones.
4. Option B describes a cactus with thick, spiny stems and no leaves, which does not match the plant in the image as the plant has leafy fronds and no spiny stems.
5. Option C describes an ostrich fern with an arching habit and tough, wiry black rhizomes, which matches the plant in the image as it has arching fronds and wiry structures.
6. Option D describes bamboo with straight stalks and green leaves, which does not match the plant in the image as the plant lacks straight stalks and bamboo-like features.
7. Based on the analysis, the plant in the image is most consistent with the description in Option C.

GPT-4.1: ✓ [bert_f1: 0.56] [rougeL_f: 0.58]

1. The question asks for the distinctive features of the plant shown in the image, and provides four options describing different types of plants. 2. Observing the image, the plant has fronds that are divided into leaflets, which is characteristic of ferns. The fronds are arching and some are turning brown, while others are still green and vibrant. 3. Option A describes a pine tree, which has needle-like leaves and cones, not matching the image. Option B describes a cactus, which has thick, spiny stems and no leaves, also not matching. Option D describes bamboo, which has straight stalks and green leaves, not seen in the image. Option C describes an ostrich fern, known for its arching fronds and tough, wiry black rhizomes, which matches the plant in the image. 4. Therefore, the correct answer is C. **Answer: C**

InternVL3-38B: ✓ [bert_f1: 0.37] [rougeL_f: 0.35]

1. The image shows a cluster of ferns with large, arching fronds. 2. The fronds have a distinct, feathery appearance with a central stem and leaflets arranged on either side. 3. Some fronds are green, while others have a brownish hue, indicating different stages of growth or decay. 4. The description of "ostrich fern with arching habit and tough, wiry black rhizomes" matches the visual characteristics of the ferns in the image. 5. The other options (pine tree, cactus, bamboo) do not match the visual features of the plant shown in the image. **Answer: C**

Fig. 8: A case of the Organism Identification task with responses from GPT-4.1 and InternVL3-38B.

Anomaly Detection

Question: Knowing that the image has 512x512 pixels, what is the type of anomaly shown at coordinates (500,293)?
Options: A: cloud_shadow B: double_plant C: planter_skip D: standing_water E: waterway F: weed_cluster G: No anomaly
Answer: G



Reasoning:

1. The question specifies that the image has dimensions of 512x512 pixels, and we are tasked with identifying the anomaly at coordinates (500,293). This means we need to focus on the bottom-right section of the image.
2. The options provided include various types of anomalies such as cloud_shadow, double_plant, planter_skip, standing_water, waterway, weed_cluster, and no anomaly.
3. Observing the image, the area at coordinates (500,293) shows a uniform texture consistent with the surrounding cultivated field, with no distinct bright green patches or irregularities.
4. The other options can be ruled out: - "cloud_shadow" would appear as a dark shadow, which is not present. - "double_plant" refers to overlapping rows of crops, which is not visible here. - "planter_skip" would show gaps in planting, which is not evident. - "standing_water" would appear as reflective or water-like areas, which are absent. - "waterway" would indicate a stream or channel, which is not visible. - "weed_cluster" is incorrect because there are no bright green patches at (500,293). - "No anomaly" is correct because the area is uniform with no irregularities.
5. Based on the analysis, there is no anomaly at (500,293). Final Answer: G

GPT-4.1: ✗ [bert_f1: 0.33] [rougel_f: 0.32]
 1. The question asks for the type of anomaly at coordinates (500,293) in a 512x512 pixel image, which is near the right edge of the image. 2. The right side of the image shows a dense, irregular patch of bright green vegetation, contrasting with the more uniform, sparse area on the left. 3. Among the options, "weed_cluster" best describes a dense, irregular patch of vegetation, as opposed to the other options which refer to water, planting errors, or the absence of anomalies. 4. Therefore, the anomaly at the specified coordinates is most consistent with a weed cluster. Answer: F

InternVL3-38B: ✗ [bert_f1: 0.19] [rougel_f: 0.22]
 1. The image shows a field with a noticeable cluster of green vegetation in the lower right corner. 2. The coordinates (500,293) fall within this cluster of green vegetation. 3. Given the options, the anomaly that matches a cluster of vegetation in an otherwise sparse field is "weed_cluster." 4. Therefore, the correct answer is F: weed_cluster. Answer: F

Fig.9: A case of the Anomaly Detection task with responses from GPT-4.1 and InternVL3-38B.

Organism Counting

Question: How many apples are there?
Answer: 6



Reasoning:

1. The question asks for the number of apples visible in the provided image.
2. Upon analyzing the image, I observe several apples scattered across the tree branches.
3. Starting from the top left, I identify one apple.
4. Moving slightly downward and to the right, I spot a second apple.
5. Further down and to the right, I locate a third apple.
6. Continuing to scan the image carefully, I find three more apples in different positions among the branches and leaves.
7. Based on this thorough analysis, the total number of apples is 6.

GPT-4.1: ✗ [bert_f1: 0.53] [rougel_f: 0.52]
 1. The question asks for the number of apples visible in the provided image. 2. I carefully examine the image to identify all the apples present. 3. I spot one apple in the upper left corner. 4. I see two apples near the bottom center of the image. 5. I notice another apple to the left of the two apples at the bottom. 6. I find one more apple slightly above and to the right of the bottom apples. 7. Summing these, there are a total of five apples visible in the image. Answer: 5

InternVL3-38B: ✓ [bert_f1: 0.36] [rougel_f: 0.25]
 1. Analyze the image to identify the apples. 2. Count the visible apples in the image. 3. There are six apples visible in the image. Answer: 6

Fig.10: A case of the Organism Counting task with responses from GPT-4.1 and InternVL3-38B.

Regional Counting

Question: Which region of the nine-palace grid do the tassels in the image mainly distribute in(Choose from Upper left region,Middle left region,Lower left region,Upper center region,Central region,Lower center region,Upper right region,Middle right region,Lower right region)? How many are there? Please format your answer as: [region],[number]. For example: Upper right region,1

Answer: Lower center region,4



Reasoning:

1. The question asks us to identify the region of a nine-palace grid where tassels are mainly distributed and count their number. The nine regions are clearly defined as Upper left, Middle left, Lower left, Upper center, Central, Lower center, Upper right, Middle right, and Lower right.
2. Observing the image, the tassels are small, light-colored structures that stand out against the green leaves.
3. By visually dividing the image into a nine-palace grid, the tassels are primarily located in the Lower center region.
4. Counting the tassels in this region, there are four visible.
5. Based on this analysis, the answer is Lower center region,4

GPT-4.1: ✓ [bert_f1: 0.59] [rougel_f: 0.51]

1. The question asks for the region of the nine-palace grid (a 3x3 grid) where the tassels in the image are mainly distributed, and how many there are. 2. The nine-palace grid divides the image into nine equal sections: upper left, upper center, upper right, middle left, central, middle right, lower left, lower center, and lower right. 3. I observe the image and identify the tassels, which are the small, light-colored, flowering parts sticking out from the green leaves. 4. I count the number of tassels visible in each region. 5. Most tassels are concentrated in the middle right region of the image, with a total of 4 tassels clearly visible there. 6. Therefore, the answer is "Middle right region,4". Answer: Middle right region,4

InternVL3-38B: ✗ [bert_f1: 0.23] [rougel_f: 0.37]

1. The image shows a dense patch of green plants with some tassels visible. 2. The tassels are located in the upper right quadrant of the image. 3. Counting the tassels in this region, there are three visible tassels. Answer: Upper right region, 3

Fig. 11: A case of the Regional Counting task with responses from GPT-4.1 and InternVL3-38B.

Morphological Statistics

Question: What is the crown diameter of the tree in the red box in the image?

Options: A: "6.00m", B: "6.96m", C: "8.48m", D: "9.52m"

Answer: A



Reasoning:

1. The question asks for the crown diameter of the tree highlighted in the red box in the image, and provides four options: 6.00m, 6.96m, 8.48m, and 9.52m.
2. The image shows a plantation with evenly spaced trees, and the tree in the red box is highlighted for measurement.
3. To determine the crown diameter, we visually assess the width of the tree's canopy. The canopy appears relatively compact compared to surrounding trees, and its horizontal spread (from one edge of the crown to the other) aligns with a narrower dimension.
4. Based on the visual scale from uniform tree spacing and the apparent size of the canopy, the most accurate estimate for the crown diameter matches 6.00m.
5. Therefore, the correct answer is A: 6.00m.

GPT-4.1: ✗ [bert_f1: 0.57] [rougel_f: 0.50]

1. The question asks for the crown diameter of the tree highlighted in the red box in the image. 2. The image shows a plantation with regularly spaced trees, and the tree in question is clearly marked. 3. The options provided are 6.00m, 6.96m, 8.48m, and 9.52m. 4. Typically, the crown diameter of oil palm trees (as seen in the image) ranges from about 6 to 8 meters, depending on age and spacing. 5. The tree in the red box appears to be of average size compared to others in the plantation, and based on the regular spacing and visual estimation, the most appropriate value among the options is 6.96m. 6. Therefore, the correct answer is B. Answer: B

InternVL3-38B: ✗ [bert_f1: 0.18] [rougel_f: 0.47]

1. The image shows an aerial view of a plantation with trees arranged in a grid pattern. 2. The red box highlights a specific tree, and we need to estimate its crown diameter. 3. By comparing the tree in the red box to the surrounding trees and considering the spacing between them, it appears to be similar in size. 4. The options provided are A: 6.00m, B: 6.96m, C: 8.48m, and D: 9.52m. 5. Given the visual comparison and typical crown diameters of such trees, 6.96m seems to be the most reasonable estimate. Answer: B

Fig. 12: A case of the Morphological Statistics task with responses from GPT-4.1 and InternVL3-38B.

Pest Recognition

Question: What pest is responsible for the damage shown in this tree bark image?
Options: A: sapsucker B: carpenter ant C: wood D: bark beetle
Answer: A



Reasoning:

1. The question asks to identify the pest responsible for the damage shown in the tree bark image, and the options provided are sapsucker, carpenter ant, wood borer, and bark beetle.
2. The image shows a tree trunk with a distinct pattern of evenly spaced, small holes arranged in horizontal rows.
3. Sapsuckers, a type of woodpecker, are known to create such patterns by pecking holes in tree bark to feed on sap and insects.
4. Carpenter ants typically create irregular tunnels inside wood, which are not visible externally as neat rows of holes.
5. Wood borers and bark beetles also create damage, but their patterns are more random or involve tunneling under the bark, not the uniform rows seen here.
6. Based on the image and the characteristic damage pattern, the pest responsible is a sapsucker. Final Answer: A

GPT-4.1: ✓ [bert_f1: 0.61] [rougel_f: 0.57]
 1. The question asks which pest is responsible for the damage shown in the tree bark image, and provides four options: sapsucker, carpenter ant, wood borer, and bark beetle. 2. Observing the image, there are rows of small, evenly spaced holes in the bark, which is a distinctive pattern. 3. Sapsuckers, a type of woodpecker, are known for creating neat rows of holes in tree bark to feed on sap and insects, while carpenter ants, wood borers, and bark beetles typically create more irregular or less visible damage. 4. Therefore, the pattern of damage in the image matches the behavior of sapsuckers. Answer: A

InternVL3-38B: ✓ [bert_f1: 0.22] [rougel_f: 0.41]
 1. The image shows a tree trunk with rows of small, evenly spaced holes. 2. These holes are characteristic of birds pecking at the bark, specifically the sapsucker, which drills holes to drink the sap. 3. The pattern of the holes is consistent with the feeding behavior of sapsuckers, rather than the random patterns typically made by wood borers or carpenter ants. 4. Bark beetles usually create more scattered and less uniform holes compared to the organized rows seen in the image. Answer: A

Fig. 13: A case of the Pest Recognition task with responses from GPT-4.1 and InternVL3-38B.

Disease Diagnosis

Question: What is the condition of the clumps in the image?
Options: A: they are large and blooming clumps B: they are moist and green clumps
 C: they are lush and vibrant clumps D: they are dry shriveled clumps
Answer: D



Reasoning:

1. The question asks about the condition of the clumps visible in the image, and provides four options describing different states of the clumps.
2. Upon analyzing the image, the clumps appear brown, shriveled, and dry, with no signs of moisture, greenness, or vibrancy.
3. Option A ("large and blooming clumps") is incorrect because the clumps are not blooming or large; they are visibly shriveled.
4. Option B ("moist and green clumps") is incorrect because the clumps are neither moist nor green; they are dry and brown.
5. Option C ("lush and vibrant clumps") is incorrect because the clumps lack vibrancy and lushness; they are shriveled and dry.
6. Option D ("dry shriveled clumps") accurately describes the condition of the clumps as seen in the image.
7. Based on the analysis, the correct answer is D.

GPT-4.1: ✓ [bert_f1: 0.49] [rougel_f: 0.41]
 1. The question asks about the condition of the clumps visible in the image. 2. Upon examining the image, the clumps appear brown, curled, and dry, rather than green, moist, or vibrant. 3. Comparing the options, A, B, and C describe clumps that are blooming, moist, or lush, which do not match the visual evidence. Option D accurately describes the clumps as "dry shriveled," which matches the appearance in the image. Answer: D

InternVL3-38B: ✓ [bert_f1: 0.30] [rougel_f: 0.28]
 1. The image shows clumps that appear to be dried and shriveled, attached to the branches of a tree. 2. These clumps are brown and lack the moisture and green coloration that would indicate they are healthy or blooming. 3. The surrounding leaves are green and healthy, which contrasts with the condition of the clumps, further indicating that the clumps are dry and shriveled. Answer: D

Fig. 14: A case of the Disease Diagnosis task with responses from GPT-4.1 and InternVL3-38B.

BioMorph Identification

Question: What species is in the image?
Options: A: Caddisfly B: Dragonfly C: Stonefly D: Mayfly
Answer: A



Reasoning:

1. The question asks to identify the species in the image from the given options: Caddisfly, Dragonfly, Stonefly, and Mayfly.
2. Observing the image, the organism appears to be encased in a structure made of small sticks or debris, which is characteristic of caddisfly larvae. Caddisfly larvae are known for constructing protective cases from materials found in their environment, such as twigs, sand, or plant matter.
3. Dragonfly, Stonefly, and Mayfly larvae do not exhibit this behavior of building cases. Instead, they have distinct body shapes and behaviors that differ from the organism shown in the image.
4. Based on the visual evidence and the unique case-building behavior, the organism in the image is identified as a caddisfly larva.
5. Therefore, the correct answer is A: Caddisfly.

GPT-4.1: ✓ [bert_f1: 0.60] [rougel_f: 0.61]
 1. The question asks to identify the species in the image from four options: Caddisfly, Dragonfly, Stonefly, and Mayfly. 2. Observing the image, there is a small aquatic insect larva on a piece of wood, and it appears to be inside a case made of small sticks or plant material. 3. Caddisfly larvae are well-known for constructing protective cases from debris such as sticks, sand, or plant material, while the larvae of dragonflies, stoneflies, and mayflies do not build such cases. 4. Therefore, based on the presence of the stick case and the aquatic environment, the species in the image is most likely a caddisfly larva. Answer: A

InternVL3-38B: ✗ [bert_f1: 0.27] [rougel_f: 0.25]
 1. The insect in the image has a long, slender body and segmented abdomen, which are characteristic features of stoneflies. 2. Stoneflies are often found near freshwater environments, such as streams and rivers, which is consistent with the setting in the image. 3. The presence of aquatic plants and the wet environment further supports the identification of the insect as a stonefly, as they are commonly found in such habitats. Answer: C

Fig. 15: A case of the BioMorph Identification task with responses from GPT-4.1 and InternVL3-38B.

Spatial Relationship

Question: Based on the provided image, if the abnormal area marked as standing_water is taken as the center, what is the spatial relationship between the abnormal area marked as weed_cluster and this central area?(The overlap ratio threshold is 50%)
Options: A: Above B: Below C: Left D: Right E: Upper Left F: Lower Left G: Upper Right H: Lower Right I: Overlap
Answer: C



Reasoning:

1. The question asks to determine the spatial relationship between the abnormal area marked as "weed_cluster" and the central area marked as "standing_water," with an overlap ratio threshold of 50%.
2. The provided image shows the "standing_water" area as a gray region in the lower-right part of the image, while the "weed_cluster" appears as sparse light green dots to the left of this gray area.
3. The two areas are spatially separated with minimal overlap (well below the 50% threshold), as the "weed_cluster" is distinctly positioned to the left of the "standing_water" region.
4. Based on the positional alignment, the spatial relationship is "Left" (meaning the "weed_cluster" is located to the left of the central "standing_water").
5. Therefore, the correct answer is C: Left.

GPT-4.1: ✗ [bert_f1: 0.46] [rougel_f: 0.47]
 1. The question asks about the spatial relationship between the abnormal area marked as "weed_cluster" and the central area marked as "standing_water," with an overlap ratio threshold of 50%. 2. I observe the image and see that the "weed_cluster" and "standing_water" areas are not distinctly separated; instead, they appear to occupy much of the same region, with significant overlap. 3. Given the overlap ratio threshold, if more than 50% of the areas coincide, the correct relationship is "Overlap." Therefore, the answer is I. Answer: I

InternVL3-38B: ✓ [bert_f1: 0.34] [rougel_f: 0.41]
 1. The image shows a landscape with a body of water on the left side and a patch of vegetation on the right side. 2. The abnormal area marked as standing_water is located near the left edge of the image, adjacent to the water. 3. The abnormal area marked as weed_cluster is situated to the right of the standing_water area. 4. Since the weed_cluster is to the right of the standing_water, the spatial relationship is that the weed_cluster is to the left of the standing_water when considering the standing_water as the center. Answer: C: Left

Fig. 16: A case of the Spatial Relationship task with responses from GPT-4.1 and InternVL3-38B.

Boundary Analysis

Question: Find the corner coordinates of the square that can enclose all the cultivated areas in the image.
Answer: [0.5904, 0.3191, 1.0, 1.0]



Reasoning:

1. The question asks for the normalized bounding box coordinates of a square that can enclose all the cultivated areas in the image. The coordinates must be normalized between 0 and 1, with (0,0) as the top-left corner and (1,1) as the bottom-right corner.
2. Observing the image, the cultivated areas are visible as rectangular patches of land with distinct patterns, primarily located in the central and right portions of the image.
3. To determine the bounding box, we identify the leftmost, topmost, rightmost, and bottommost extents of the cultivated areas. These areas are roughly in the middle of the image horizontally and vertically.
4. Normalizing the coordinates involves estimating the relative positions of these extents within the image dimensions. The cultivated areas span approximately from 59% to 100% of the width (x-axis) and from 31% to 100% of the height (y-axis).
5. The bounding box is defined as [xmin, ymin, xmax, ymax] = [0.59, 0.31, 1.0, 1.0].

GPT-4.1: ✗ [bert_f1: 0.46] [rougeL_f: 0.41]

1. The question asks for the normalized coordinates of a square bounding box that can enclose all the cultivated areas in the image. 2. "Cultivated areas" refer to the fields or plots of land that show signs of agricultural activity, typically visible as patterned or organized sections of land. 3. Observing the image, the cultivated areas are mostly located in the central and right portions, with some extending towards the left near the buildings. The leftmost part of the image contains industrial structures, while the right side and center show fields with visible rows and patterns. 4. To enclose all cultivated areas, the bounding box should start just above the topmost field and end just below the bottommost field, while also covering the leftmost and rightmost extents of the fields. 5. The top-left corner of the bounding box should be slightly inside from the left edge (to avoid including the industrial buildings) and slightly down from the top edge (to include the topmost field). 6. The bottom-right corner should be just before the right edge and just above the bottom edge, covering the furthest extents of the cultivated land. 7. By visually estimating the normalized coordinates: xmin = 0.13 (left edge of cultivated area) xmax = 0.87 (right edge of cultivated area) ymin = 0.23 (top edge of cultivated area) ymax = 0.93 (bottom edge of cultivated area). 8. These coordinates form a square that encloses all the cultivated areas visible in the image. Answer: 0.13,0.23,0.87,0.93

InternVL3-38B: ✗ [bert_f1: 0.36] [rougeL_f: 0.34]

1. Identify the boundaries of the cultivated areas in the image. The cultivated areas are the brown patches on the right side of the image. 2. Determine the leftmost point of the cultivated areas. This point is approximately 25% from the left edge of the image. 3. Determine the topmost point of the cultivated areas. This point is approximately 25% from the top edge of the image. 4. Determine the rightmost point of the cultivated areas. This point is approximately 95% from the left edge of the image. 5. Determine the bottommost point of the cultivated areas. This point is approximately 95% from the top edge of the image. 6. Combine these points to form the bounding box coordinates: [0.25, 0.25, 0.95, 0.95]. Answer: 0.25, 0.25, 0.95, 0.95

Fig. 17: A case of the Boundary Analysis task with responses from GPT-4.1 and InternVL3-38B.

Area Evaluation

Question: "Given that the actual geographical area of the entire image is 42025.0 square meters, what is the approximate tree-covered area of the ecosystem(Can be calculated based on coverage ratio)?
Options: A: [39700-39800]square meters B: [9500-9600]square meters C: [10300-10400]square meters D: [2600-2700]square meters
Answer: B



Reasoning:

1. The question provides the total geographical area of the image as 42,025 square meters and asks for the approximate tree-covered area based on the coverage ratio.
2. Observing the image, tree-covered areas are concentrated along the riverbank, around houses, and in open spaces, but they do not form a majority.
3. The tree-covered area appears to occupy a moderate portion, estimated at around 22.6-22.8% of the total area.
4. Calculating this percentage of 42,025 square meters: $0.227 * 42,025 = 9540$. This value is close to the range [9500-9600] square meters.
5. Comparing this result with the options, Option B ([9500-9600] square meters) is the most appropriate choice. 6. Therefore, the answer is B.

GPT-4.1: ✗ [bert_f1: 0.59] [rougeL_f: 0.51]

1. The question provides the total geographical area of the image as 42,025.0 square meters and asks for the approximate tree-covered area based on the coverage ratio. 2. By visually analyzing the image, the tree-covered regions are mainly along the water, scattered throughout the residential lots, and along the roads, but they do not dominate the entire image. The majority of the area consists of open land, houses, roads, and water. 3. Estimating the tree coverage, it appears to be roughly 25% of the total area. Calculating 25% of 42,025 gives approximately 10,506 square meters. Among the options, the range [10,300-10,400] square meters (Option C) is the closest to this estimate. 4. Therefore, the correct answer is C. Answer: C

InternVL3-38B: ✗ [bert_f1: 0.16] [rougeL_f: 0.45]

1. The image shows a landscape with a significant portion covered by trees, particularly on the left side and around the houses. 2. The total area of the image is given as 42025.0 square meters. 3. By visually estimating the tree coverage, it appears that trees cover roughly a quarter to a third of the total area. 4. Calculating a quarter of 42025.0 square meters gives approximately 10506.25 square meters. 5. This value falls within the range of option C: [10300-10400] square meters. 6. Therefore, option C is the most appropriate choice based on the estimated tree coverage ratio. Answer: C

Fig. 18: A case of the Area Evaluation task with responses from GPT-4.1 and InternVL3-38B.

Agri-Tools

Question: What is the intended function of this device in a farming context?
Options: A: To generate soothing water sounds for decorative use. B: To scare off animals that might harm crops. C: To deter insects and pests from feeding on plants. D: To store and redirect rainwater for agricultural use. E: To lure wildlife into a designated zone for monitoring.
Answer: B



Reasoning:

1. The question asks for the intended function of the device in a farming context, and provides five options to choose from.
2. The image depicts a traditional Japanese water feature known as a "shishi-odoshi," which consists of bamboo pipes and a pivoting mechanism that creates a sound when water fills and tips the bamboo.
3. Option A suggests the device is for decorative use, but while the device does produce soothing sounds, its primary purpose is not decoration in a farming context.
4. Option B suggests the device is used to scare off animals that might harm crops. This aligns with the historical function of the "shishi-odoshi," which was designed to create noise to deter animals such as deer or boars from entering crop areas.
5. Option C suggests the device deters insects and pests, but the mechanism of the "shishi-odoshi" is not effective against small pests like insects.
6. Option D suggests the device stores and redirects rainwater, but the "shishi-odoshi" does not have a storage or redirection function for agricultural irrigation.
7. Option E suggests the device lures wildlife for monitoring, but the noise produced by the "shishi-odoshi" is intended to repel wildlife, not attract it.
8. Based on the analysis, the correct answer is Option B, as the primary function of the device in a farming context is to scare off animals that might harm crops.

GPT-4.1: ✓ [bert_f1: 0.45] [rougeL_f: 0.44]
 1. The question asks about the intended function of the device in a farming context, and provides several options related to water, sound, animal deterrence, and wildlife management. 2. The image shows a traditional Japanese bamboo water feature known as a "shishi-odoshi," which consists of a pivoting bamboo tube that fills with water and then tips over, making a knocking sound as it strikes a rock or another object. 3. The primary purpose of a shishi-odoshi in a farming or garden context is to scare off animals (such as deer or birds) that might harm crops, using the sudden sound to startle them; therefore, option B is the correct answer. **Answer:** B

InternVL3-38B: ✗ [bert_f1: 0.22] [rougeL_f: 0.28]
 1. The image shows a bamboo water system with a stone basin, which is commonly used in traditional farming to manage water. 2. The setup suggests a method for collecting and redirecting water, likely for irrigation purposes. 3. The presence of bamboo pipes and the stone basin indicates a functional design for water storage and distribution rather than purely decorative or pest control purposes. **Answer:** D

Fig. 19: A case of the Agri-Tools task with responses from GPT-4.1 and InternVL3-38B.

Agri-Methods

Question: In this image, what task is being performed?
Options: A: Watering the crops. B: Mixing organic matter. C: Ploughing the soil. D: Harvesting the grain. E: Transporting harvested crops.
Answer: C



Reasoning:

1. The question asks to identify the task being performed in the image, and the options provided include various agricultural activities.
2. Observing the image, a buffalo is being used to pull a plow, which is a tool designed to break and turn over soil. This is a clear indication of soil preparation for planting crops.
3. Option A, "Watering the crops," is incorrect because there is no visible water or irrigation activity in the image.
4. Option B, "Mixing organic matter," is incorrect because the activity shown is focused on ploughing, not mixing compost or organic material.
5. Option D, "Harvesting the grain," is incorrect because there are no crops being harvested in the image; the field is bare and being prepared for planting.
6. Option E, "Transporting harvested crops," is incorrect because there are no harvested crops visible, nor is there any transportation activity occurring.
7. Option C, "Ploughing the soil," is correct because the image clearly shows the buffalo pulling a plow to prepare the soil for planting.
8. Based on the analysis, the correct answer is C.

GPT-4.1: ✓ [bert_f1: 0.38] [rougeL_f: 0.43]
 1. The question asks what task is being performed in the image, and provides five options related to agricultural activities. 2. In the image, there is a large animal (a water buffalo) harnessed to a wooden plow, with two people guiding and controlling the animal and the plow. 3. The soil in the foreground appears freshly turned, indicating that the animal is being used to break up and turn over the soil, which is characteristic of ploughing. 4. The other options (watering, mixing organic matter, harvesting, transporting crops) do not match the activity shown, as there is no visible water, organic matter being mixed, harvested grain, or transportation of crops. 5. Therefore, the correct answer is ploughing the soil. **Answer:** C

InternVL3-38B: ✓ [bert_f1: 0.28] [rougeL_f: 0.33]
 1. The image shows a water buffalo pulling a plow through a field, which is a common method for preparing soil for planting. 2. The presence of the plow and the action of turning the soil indicate that the task being performed is related to soil preparation. 3. The individuals in the image are guiding the water buffalo and plow, further confirming that the task is ploughing the soil. **Answer:** C

Fig. 20: A case of the Agri-Methods task with responses from GPT-4.1 and InternVL3-38B.

Management Decisions

Question: What action should be taken to manage the tree shown in the image?
Options: A: apply fertilizer to the soil B: trim the branches regularly
 C: water the tree frequently D: remove the tree and its roots

Answer: D



Reasoning:

1. The question asks for the most appropriate action to manage the tree shown in the image, and provides four options: applying fertilizer, trimming branches, watering frequently, or removing the tree and its roots.
2. Upon analyzing the image, the tree appears to have significant damage to its trunk, with visible decay or splitting. This suggests that the tree may be unhealthy or structurally compromised.
3. Applying fertilizer (Option A) would not address the structural damage or decay visible in the tree trunk. Fertilizer is typically used to promote growth and health in trees that are otherwise intact.
4. Trimming branches regularly (Option B) is a maintenance action for healthy trees or those with overgrown branches, but it does not address the core issue of trunk damage.
5. Watering the tree frequently (Option C) is beneficial for trees suffering from drought stress, but the image does not indicate drought stress; instead, the issue is structural damage to the trunk.
6. Removing the tree and its roots (Option D) is the most appropriate action because the visible damage to the trunk suggests the tree may pose a safety risk or is beyond recovery. Removing the tree would prevent potential hazards such as falling limbs or the tree collapsing.
7. Based on the analysis, Option D is the correct choice.

GPT-4.1: ✘ [bert_f1: 0.39] [rouge1_f: 0.39]

1. The question asks about the appropriate action to manage the tree shown in the image. 2. The image shows a healthy tree trunk with no visible signs of disease or severe damage, and the surrounding area appears to be a maintained garden bed. 3. Among the options, applying fertilizer (A) or watering frequently (C) are not specifically necessary based on the visible condition of the tree, and removing the tree (D) is not warranted as the tree appears healthy. 4. Regularly trimming the branches (B) is a standard and recommended practice for tree maintenance to promote healthy growth, remove dead or diseased branches, and maintain shape. 5. Therefore, the most appropriate action is to trim the branches regularly. Answer: B

InternVL3-38B: ✔ [bert_f1: 0.30] [rouge1_f: 0.46]

1. The tree in the image appears to be dead or dying, as indicated by the lack of leaves and the dry, brittle branches. 2. Applying fertilizer (Option A) or watering frequently (Option C) would not help a tree that is already dead or dying. 3. Trimming branches (Option B) is unnecessary for a dead tree and does not address the root issue. 4. Removing the tree and its roots (Option D) is the most appropriate action to prevent potential hazards and to prepare the area for future landscaping. Answer: D

Fig. 21: A case of the Management Decisions task with responses from GPT-4.1 and InternVL3-38B.